

A MICROWAVE DOPPLER TECHNIQUE FOR  
VEHICLE SPEED DETERMINATION

by Neil Cameron Martin

A dissertation submitted to the Faculty of Engineering at the University of Cape Town for the degree of Master of Science in Electrical and Electronic Engineering.

CAPE TOWN, APRIL 1987.

The University of Cape Town has been given the right to reproduce this thesis in whole or in part. Copyright is held by the author.

The copyright of this thesis vests in the author. No quotation from it or information derived from it is to be published without full acknowledgement of the source. The thesis is to be used for private study or non-commercial research purposes only.

Published by the University of Cape Town (UCT) in terms of the non-exclusive license granted to UCT by the author.

## DECLARATION

I declare that this dissertation is my own unaided work. It is being submitted for the degree of Master of Science in Engineering at the University of Cape Town. It has not been submitted before for any degree or examination at this or any other university.

Signed by candidate

N C Martin  
(Signature of Candidate)

25th day of April 1987

## ABSTRACT

Conventional Microwave Doppler Speed Measurement systems have long been considered unusable in many situations. In this dissertation a novel technique for speed measurement is presented which eliminates some of the problems associated with conventional systems, in particular the problem of vehicle identification. It is shown how a 'capture area' may be defined. Only the speeds of vehicles within the capture area are measured. A prototype speed measuring instrument was designed and constructed. The instrument was shown to work as predicted and the the notion of the 'capture area' was proved.

## ACKNOWLEDGEMENTS

I would like to thank the following people:

My supervisor, Prof. B. J. Downing for his support and encouragement,

Mr J. Greene for his helpful advice,

The CSIR and Plessey S.A. for their financial assistance.

## TABLE OF CONTENTS

	Page Number
DECLARATION	i
ABSTRACT	ii
ACKNOWLEDGEMENTS	iii
CONTENTS	iv
1. INTRODUCTION	1
1.1 THE MEASUREMENT OF VEHICLE SPEEDS	1
1.2 INTRUSIVE MEASUREMENTS OF SPEED	2
1.2.1 CO-OPERATIVE SPEED MEASUREMENTS	2
1.2.2 NON-CO-OPERATIVE, INTRUSIVE METHODS	3
1.3 NON-INTRUSIVE MEASUREMENTS OF VEHICLE SPEED	4
1.3.1 INTRODUCTION	4
1.3.2 LIGHT AND LASER METHODS	5
1.3.3 VIDEO METHODS	7
1.3.4 ACOUSTIC AND OTHER METHODS	8
1.4 OBJECTIVE	8
1.5 LAYOUT OF DISSERTATION	9
2. REVIEW OF CONVENTIONAL MICROWAVE SPEED MEASURING INSTRUMENTS	10
2.1 THE DOPPLER EFFECT	10
2.2 INTRODUCTION	10
2.3 CONVENTIONAL SYSTEM FUNCTIONAL OVERVIEW	11
2.4 CONVENTIONAL SYSTEM SHORTCOMINGS	15
2.4.1 THE CSIR REPORT	15
2.4.2 THE VEHICLE IDENTIFICATION PROBLEM	17

3. PROPOSED SYSTEM FOR MICROWAVE SPEED MEASUREMENT	19
3.1 INTRODUCTION TO NEW TECHNIQUE	19
3.2 THE SIGNAL PROCESSING ALGORITHM	20
3.3 THE CAPTURE AREA	24
4. PRACTICAL IMPLEMENTATION	29
4.1 INTRODUCTION	29
4.2 SYSTEM OVERVIEW	29
4.3 SIGNAL PROCESSOR	30
4.3.1 SIGNAL PROCESSING CONSIDERATIONS	30
4.3.2 THE DEVELOPMENT OF DEDICATED SIGNAL PROCESSORS	31
4.4 MICROWAVE SOURCES	32
4.4.1 FREQUENCY	32
4.4.2 RANGE, ANTENNA GAIN, POWER AND SENSITIVITY	33
4.5 INTERFACING CIRCUITRY	34
4.5.1 INTRODUCTION	34
4.5.2 DYNAMIC RANGE	34
5. SOURCE	36
5.1 MICROWAVE OSCILLATORS	36
5.1.1 INTRODUCTION	36
5.1.2 CAVITY GUNN OSCILLATORS	37
5.2 PROTOTYPE OSCILLATOR	38
5.2.1 GUNN DIODE CHARACTERISTICS	38
5.2.2 OSCILLATOR DESIGN	39
5.3 MICROWAVE MIXERS	40
5.3.1 SELF MIXING OSCILLATORS	40
5.3.2 MIXER DIODES	41
5.4 PROTOTYPE MIXER	41
5.4.1 MIXER DIODE CHARACTERISTICS	41
5.4.2 MIXER DESIGN	42
5.4.3 OSCILLATOR AND MIXER COUPLING	44
5.5 BIAS	44
5.5.1 GUNN OSCILLATOR BIAS	44

5.5.2 MIXER BIAS	45
5.6 NOISE CONSIDERATIONS	46
5.6.1 OSCILLATOR NOISE	46
5.6.2 MIXER NOISE	48
5.7 ANTENNA	50
5.7.1 INTRODUCTION	50
5.7.2 ANTENNA GAIN	51
5.7.3 HORN ANTENNA DESIGN	52
5.8 OSCILLATOR FREQUENCIES	54
5.9 DOPPLER FREQUENCIES	56
6. INTERFACING CIRCUITRY	57
6.1 INTERFACING CONSIDERATIONS	57
6.1.1 INTRODUCTION	57
6.1.2 TMS32010 COMMUNICATION LINES	58
6.1.3 MODULAR DESIGN	59
6.2 DOPPLER PRE-AMPLIFIER	60
6.3 CABLES	62
6.4 AUTOMATIC GAIN CONTROL	63
6.4.1 AGC AMPLIFIER REQUIREMENTS	63
6.4.2 AGC CIRCUIT	64
6.5 MULTIPLEXOR	67
6.6 ANTI-ALIASING FILTER	68
6.6.1 INTRODUCTION	68
6.6.2 ANTI-ALIASING FILTER REQUIREMENTS	69
6.6.3 FDNR FILTERS	70
6.6.4 FILTER REALISATION	71
6.7 ANALOG TO DIGITAL CONVERTER	74
6.8 DISPLAY CARD	76
7. SIGNAL PROCESSING	78
7.1 THE FOURIER TRANSFORM	78
7.1.1 INTRODUCTION	78
7.1.2 THE DISCRETE FOURIER TRANSFORM	78
7.1.3 THE FAST FOURIER TRANSFORM	80
7.1.4 THE DFT AND FFT FOR REAL DATA	80

7.2	POWER SPECTRAL ESTIMATION	81
7.2.1	INTRODUCTION	81
7.2.2	LEAKAGE AND WINDOWING	81
7.2.3	THE 'PICKET-FENCE' EFFECT	83
7.3	SIGNAL PROCESSING HARDWARE	85
7.3.1	EVALUATION MODULE	85
7.3.2	OUT GENERATION	86
7.4	INTRODUCTION TO THE SIGNAL	
	PROCESSING REQUIREMENTS	87
7.4.1	SIGNAL PROCESSING BLOCK DIAGRAM	87
7.4.2	THE FFT ALGORITHM	88
7.4.2.1	THE COOLEY-TUKEY ALGORITHM	88
7.4.2.2	THE CHOICE OF N AND $F_S$	90
7.4.2.3	FFT FLOWCHART	91
7.4.3	DATA ACQUISITION	93
7.4.4	WINDOWING	94
7.4.5	CONVERSION TO POWER SPECTRA	94
7.4.6	SELECTING THE DISPLAYED SPEED	95
7.5	SIGNAL PROCESSING SOFTWARE	96
7.5.1	INTRODUCTION	96
7.5.1.1	PROGRAM EFFICIENCY	96
7.5.1.2	MEMORY ALLOCATION	97
7.5.1.3	DATA REPRESENTATION	98
7.5.2	TMS32010 CODE	98
7.5.2.1	SOFTWARE LISTING	98
7.5.2.2	SUBROUTINE DESCRIPTIONS	98
7.5.3	PROCESSING SPEED	101
8.	SPEED MEASURING INSTRUMENT OPERATION	102
8.1	INTRODUCTION	102
8.2	INSTRUMENT PERFORMANCE	102
8.2.1	TEST CONFIGURATION	102
8.2.2	MEASURED CAPTURE RANGE	103
8.2.3	VEHICLE DISCRIMINATION	104
8.2.4	SPURIOUS SPEED READINGS	105
8.2.5	SIGNAL FLUCTUATIONS	105

8.3 DEVIATION FROM THEORETICAL PERFORMANCE	106
8.3.1 FACTORS AFFECTING THE SIZE OF THE CAPTURE AREA	106
8.3.2 SPECTRAL SMEARING	108
8.3.3 CAUSES OF SPURIOUS SPEED READINGS	109
8.3.4 CAUSES OF SIGNAL AMPLITUDE FLUCTUATIONS	111
8.4 SYSTEM SHORTCOMINGS	111
8.5 POSSIBLE IMPROVEMENTS TO THE SYSTEM	113
9. CONCLUSION	115
REFERENCES	117
APPENDIX A : A SUMMARY OF THE FINDINGS OF THE CSIR REPORT.	
APPENDIX B : DIAGRAMS FOR THE CONSTRUCTION OF THE MICROWAVE SOURCE, ANTENNA AND ACCESORIES.	
APPENDIX C : TMS32010 SOFTWARE FOR SPEED MEASUREMENT SYSTEM.	
APPENDIX D : PART OF THE DATA SHEET OF THE TMS32010.	
APPENDIX E : PUBLISHED WORK AND PATENT.	

## CHAPTER 1 : INTRODUCTION

### 1.1 THE MEASUREMENT OF VEHICLE SPEEDS

The measurement of the speed of vehicles can be broadly classified under two headings:

- i) Intrusive measurement techniques; and
- ii) Non-intrusive methods.

Under the heading of the Intrusive measurement of vehicle speed is included those methods in which the vehicle co-operates with the measuring system, by, for instance, carrying a transmitter, sensor, transponder, or other object that aids in the measurement process. Also included in this category of measurement is the method whereby parallel lines are stretched across the road. This method is discussed in Section 1.2.2.

In speed measurement applications where it is desirable that the driver of the vehicle is unaware that a speed measurement is being made, in the case, for instance, of "speed trapping" by Traffic Police, non-intrusive methods are preferable. Under this heading are included microwave, laser and video methods, as well as a host of other measurement schemes. Some of these methods are discussed in Section 1.3.

This dissertation is primarily concerned with the non-intrusive, non-co-operative measurement of speed by microwave techniques. Before a detailed study of this technique is made, however, it is worthwhile to briefly

examine other methods available for the measurement of vehicle speed.

## 1.2 INTRUSIVE MEASUREMENTS OF SPEED

### 1.2.1 CO-OPERATIVE SPEED MEASUREMENTS

In recent years much attention has been given to the measurement of the speed of vehicles in terms of its application to automated ground control systems, in particular the Automated Highway System [1]. Saxton [2] showed that many of the problems associated with the AHS could be eased if the active elements of the system, including the components of the speed measurement system, were vehicle based. The majority of tests reported in the literature [3,4] do, in fact, use vehicle based components - thus making these systems vehicle co-operative, and it seems that in the future this trend will continue.

Intrusive vehicle speed measurements are considerably easier to implement than non-intrusive ones, and many techniques are available for such measurements. Microwave, laser, acoustic and magnetic active devices have all been used in co-operative speed measurements [5]. In these cases an active or passive system element is carried by the vehicle. Microwave systems, where the active microwave transmitter is carried by the vehicle, are popular with experimentors of AHS. This is primarily because one of the greatest problems of speed measurement by microwave techniques, that of vehicle identification [see Section 2.4.2], is eliminated if the active device is vehicle-borne.

### 1.2.2 NON-CO-OPERATIVE, INTRUSIVE METHODS

The application of vehicle speed measurement systems to AHS is a relatively new one, as AHS has only become feasible since the introduction of fast, dedicated computers. The greatest application of ground based speed measuring systems has always been, and still is, "Speed-Trapping" by Traffic Police. In this application the vehicle does not co-operate with the measurement and all components of the measurement system must be external to the vehicle whose speed is being measured.

At the present time in South Africa the instruments that are almost exclusively used by Traffic Police are based on the principle of stretching parallel lines across the road. Vehicle tyres crossing the lines cause a capacitance change, a change in pressure, a piezo-electrically induced voltage or some other measurable change to a parameter of the line. The time between the change that occurs in each line is measured and this time, together with the accurately known distance between the lines, enables the speed to be calculated. The brand names Gatsometer and Truvelo have become well known.

The method of parallel lines is a popular one because of the small number of error readings it produces in comparison with other methods of speed measurement available. There are still, however, a large number of disadvantages associated with this technique of measuring speed. The first is that the nailing of the lines to the road is a laborious procedure, as it must be done accurately if the measured speed error is to be low. If the lines are 1.5m apart (the distance between the lines of the Truvelo) their position must be accurate to within 7.5mm to achieve a speed error of less than 1km/h at a speed of 200km/h. Because this accuracy is difficult to attain, the generally accepted

operating procedure is to place the lines slightly further apart than 1.5m so as to give the vehicle a 3% "leeway". Thus the instrument will read 3% low in speed so that if the lines do move slightly it is unlikely that the instrument will read a vehicle's speed as higher than its true speed.

The setting up of such a system takes between 30 and 45 minutes and is not only time consuming but also dangerous to the Traffic Policemen involved. A further disadvantage of this system is that because the lines come into contact with vehicle tyres they are easily and frequently damaged, either by vehicles braking suddenly, or simply from wear. The lines are expensive and the Johannesburg Traffic Authority alone spends more than R5000 per month on the replacement of lines for their speed measurement systems.

One important advantage that this method has over many other methods of speed measurement is that the measurement area is relatively small. This means that it is easy to identify which vehicle's speed has been measured. The method of parallel lines is particularly suited to areas where the traffic density is relatively high.

### **1.3 NON-INTRUSIVE MEASUREMENTS OF VEHICLE SPEED**

#### **1.3.1 INTRODUCTION**

Non-intrusive speed measurement systems are generally more complex than intrusive ones as no part of the measuring equipment comes into contact with the vehicle.

The most important non-intrusive speed measuring systems are based on:

uneven radiator grills. Placing the beams near road level does not alleviate the problem as "knobbly" tyres could produce the same effect. At the CSIR road test facility in Pretoria a similar system to the one just described is used. Laser beams are employed. To reduce the problem of vehicle "bounce" a vertical board is fixed to the front of the vehicle so that this board is always the first object to block the laser beam. Such a system is obviously a vehicle co-operative one.

The recent availability of low cost solid state lasers make the laser a possibility for speed measurement applications. The field of laser velocimetry is a well established one and is very important in aerodynamic flow studies [6,7].

The advantage of lasers in speed measurement applications is that a virtual point source of light can be focussed on a vehicle, eliminating the identification problem which is prevalent in many speed measurement systems [see Section 2.4.2].

Two laser speed measurement techniques exist:

- i) Doppler methods, and
- ii) Tellurometer methods

Doppler techniques are the basis of laser velocimetry. In laser doppler techniques for speed measurement the laser beam is directed onto the vehicle and the reflected signal is mixed with the incident signal. The mixing results in a doppler signal whose frequency is proportional to the speed of the vehicle. If the mixing takes place at baseband, ie at light frequencies, then high precision is possible, as the resulting doppler frequencies are high. A mixer at light frequencies is, however, prohibitively expensive and

it is more usual to modulate the source so that the mixing can take place at a more convenient frequency. This is, of course, at the cost of lower precision.

In the Tellurometer technique the distance between the vehicle and the stationary instrument is measured. Some time later the distance is measured again. The difference in distances together with the time that elapsed between measurements enables the speed to be calculated.

The greatest disadvantage of the laser is that unless the vehicle co-operates by carrying a reflective surface, high power is needed to ensure a large enough reflected signal. The power needed exceeds public safety standards set for the use of laser equipment.

### **1.3.3 VIDEO METHODS**

Recent advances in the field of image processing have made speed measurement by 'Video' means a possibility. The advances in this field have come as a direct result of the vast increase in processing power offered by fast dedicated microcomputers [see Section 4.3.2]. The recent introduction of parallel processors will further enhance this field. Speed measurements are made by measuring the distance a vehicle has travelled between successive frames of the video image.

The advantage of the video method is that a permanent record of the activity on the road is kept, and the equipment may be incorporated into a road traffic control system.

Disadvantages of the video method at the present time are:

- (i) It is still an expensive means of measuring speed; and
- (ii) The equipment is physically large so that only fixed installations are practical.

#### **1.3.4 ACOUSTIC AND OTHER METHODS**

Over the years a number of other methods for measuring the speed of vehicles have been proposed. Many of these used correlation techniques incorporated into systems based on the parallel line method. In such speed measurement systems acoustic devices could be used as the sensors, and a signal processing unit used to calculate the time of travel between the sensors. In 1975 Jakus and Coe [8] proposed a speed measurement technique using a single acoustic sensor and analysing the doppler effect in the vehicle noise.

One problem facing all designers of speed measuring equipment until recently was the lack of cheap processing power. With the current availability of processing power in the form of dedicated signal processors on a chip, a re-evaluation of many of the techniques previously rejected is now possible.

#### **1.4 OBJECTIVE**

It is the objective of this dissertation to re-evaluate the measurement of the speed of vehicles by Microwave Doppler techniques. An improvement to the system as it presently exists will be proposed. A practical realisation of the proposed system is presented, and its performance analysed and compared to existing Microwave Doppler instruments.

## 1.5 LAYOUT OF DISSERTATION

The remainder of this dissertation consists of 8 chapters.

In Chapter 2 a detailed study of Microwave Doppler speed measuring instruments currently available is made. Their advantages and failings are pointed out.

In Chapter 3 a new method for measuring speed with Microwave Doppler techniques is proposed. The theory of the system is presented and theoretical improvements over existing systems are shown.

Chapters 4 through to 8 deal with the practical implementation of the system. The practical realisation is introduced in Chapter 4 and the individual aspects of the Microwave source, analog circuitry, signal processing and system testing are dealt with in Chapters 5 to 8.

Chapter 9 concludes this dissertation.

## CHAPTER 2 : REVIEW OF COVENTIONAL MICROWAVE SPEED MEASURING INSTRUMENTS

### 2.1 THE DOPPLER EFFECT

When an electromagnetic or acoustic wave is reflected from a moving object, it undergoes a change in frequency. This frequency change is known as the Doppler effect and the change in frequency, or Doppler frequency, is given by:

$$f_d = \frac{2v}{\lambda}$$

where  $v$  : velocity of moving object  
 $\lambda$  : wavelength of incident signal

If the incident signal  $f_0$  and the reflected signal  $f_1$  are combined in a single-ended mixer, then the frequencies  $f_0+f_1$  and  $f_0-f_1$  will result. The doppler frequency,  $f_d$ , is equal to  $[f_0-f_1]$ . This result has no sign associated with it: that is there is no information present about whether the object is moving towards or away from the transmitter.

If a microwave transmitter is used, operating in the X or K frequency bands, then the doppler shifts resulting from moving vehicles fall conveniently in the audio frequency band.

### 2.2 INTRODUCTION

Microwave doppler techniques have been used to measure the speed of vehicles since the invention of radar. It was, however, only after cheap, solid state microwave devices

became available in the late 1960's that commercial Doppler Speed measuring instruments were manufactured.

The public have doubted the integrity of these instruments almost since their inception. Equipment manufacturers were reluctant to admit the failings of the systems and in the early years a "radar" speed reading was acceptable evidence in Law Courts around the world. In the latter half of the 1970's, however, engineers began to join in the "fight" against 'police radar', as it came to be known [9,10,11,12,13]. Law Courts began to reject radar speed readings and world-wide microwave doppler speed measuring instruments came under review. In South Africa this review took the form of a CSIR investigation. The findings of this report are discussed in Section 2.4.1.

### 2.3 CONVENTIONAL SYSTEM FUNCTIONAL REVIEW

In order to appreciate the problems associated with microwave speed meters in their present form, a review of the operation of these instruments is necessary.

The schematic diagram and road geometry of a typical Doppler speed measuring instrument is shown in Figure 2.1.

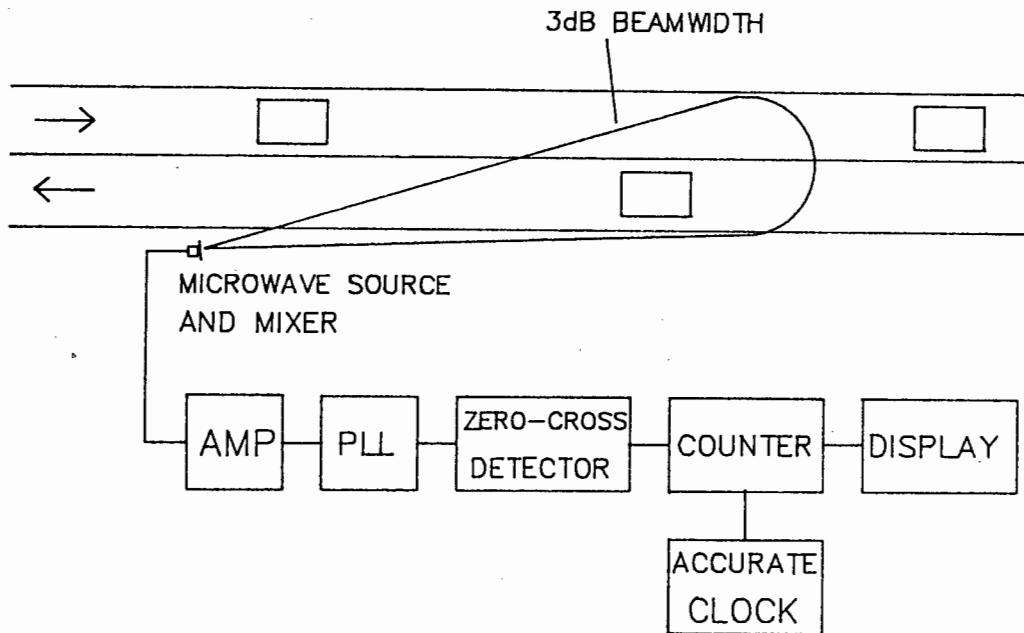


FIGURE 2.1 CONVENTIONAL DOPPLER SPEED MEASURING INSTRUMENT  
BLOCK DIAGRAM

The transmitter and receiver share a common antenna. The Microwave source consists of a Gunn oscillator of frequency 10.525 GHz or 24.150 GHz, the two frequencies approved by the FCC of the USA for microwave speed measuring equipment. This oscillator is mounted in a cavity together with a mixer. When the fundamental frequency and doppler shifted return are mixed together, a doppler difference signal whose frequency is proportional to the vehicle speed results.

The doppler signal, which is assumed to be sinusoidal, is then fed into a phase locked loop. The phase locked loop is a desirable feature of this system as it provides a certain amount of noise rejection.

The resulting signal is squared with a zero-crossing detector before being fed to a counter gated with an accurate clock. The counter output is then passed to a display which is typically of the 7-segment LED type. Most systems have a resolution of 1km/h, and in no country does the law require that vehicle speeds be measured more accurately than this.

The source power and antenna gain are such that the system is capable of long range : 1 km for a "standard" car and much more for a large truck. One commercial system obtained for test purposes, the Digidar IIK, had a measured output power of 100mW @ 10.525 Ghz and an antenna gain of 26dB. Although high power and high gain have advantages in terms of long range performance and a high signal to noise ratio, they also have disadvantages as will be shown in Section 2.4.2.

Noise "contamination" of the doppler signal is present in two forms in this system:

- i) Normal electrical noise and,
- ii) Unwanted doppler signals.

Most of the electrical noise present in the doppler signal originates from the Mixer Diode. This noise is amplified together with the low-level doppler signals.

Unwanted doppler signals arise from vehicles other than the vehicle whose speed is being measured. As these signals are unwanted, they will be considered as noise.

A system incorporating a phase locked loop is able to make speed measurements in the presence of both types of noise. Rejection of random noise (such as electrical noise) is an

inherent property of the phase locked loop. In the case of doppler signal 'noise' the phase locked loop can be made to select either the largest amplitude signal (the usual case), or the highest frequency one (and thus the fastest vehicle), depending on the instrument.

This system has the potential to be a highly accurate method of measuring the speed of vehicles. The system accuracy depends primarily on the accuracy of :

i) The frequency of the clock gating the counter.

ii) The frequency of the microwave source

To ensure frequency stability, the clock gating the counter is usually quartz-crystal controlled. The typical figure for the frequency stability of a quartz-crystal oscillator, 10-20 ppm over the operating temperature range, is more than adequate for 'police' speed measurement purposes.

Frequency drift in the oscillator is a more serious problem. Although the cost of frequency stabilised microwave oscillators has been steadily decreasing, stabilised microwave oscillators are still too expensive to be incorporated in speed measuring equipment.

At X-band (10.525 GHz) the frequency of the source must drift by more than 50 MHz to cause a speed error of greater than 1 km/h at a speed of 200 km/h. Similarly at K-band the frequency must change by more than 120 MHz to cause the same error. According to FCC regulations speed measuring equipment may operate at 10.525 GHz +/- 25MHz or 24.150 GHz +/- 50 MHz. Thus if the sources are operating within FCC regulations they will not affect the accuracy of the instrument.

Cavity Gunn oscillators typically exhibit a frequency-temperature characteristic of less than 2 MHz per °C [see Section 5.8]. Thus under normal operating temperatures the source frequency does not drift significantly from its nominal value.

## 2.4 CONVENTIONAL SYSTEM SHORTCOMINGS

### 2.4.1 THE CSIR REPORT

In 1978, at the request of the South African Traffic Authorities, the NITR division of the CSIR, headed by B. van der Riet, conducted an investigation into the Microwave Doppler Speed Measuring Instruments that were in use at the time [14]. Similar studies have been conducted elsewhere in the world both before and since the CSIR one. It is the findings of the CSIR report, however, that are discussed here, as this report was both comprehensive and applicable to the South African context.

Before any official investigation was made, microwave doppler instruments were suspected of giving incorrect speed readings due to a number of factors. These included :

- i) Vehicle vibration,
- ii) Moving objects on vehicles such as wheels, hubcaps, cooling fans, windscreen wipers etc,
- iii) Multiple reflections between vehicles and other objects,
- iv) Deflection of the microwave beam,

- v) Electromagnetic interference (EMI),
- vi) The presence of birds or other objects in the beam,
- vii) Instrumental inaccuracies,
- viii) Inability to identify which vehicle's speed is being measured in a multiple vehicle situation.

All of the factors listed above were examined by van der Riet. The procedure they adopted in order to ascertain whether or not a certain factor influenced speed measurements was one in which they attempted to duplicate the influencing factor.

A table summarising the results of their experiments is shown in Appendix A.

Van der Riet concluded that the major problem that exists with microwave speed measuring equipment is one of vehicle identification. They rejected the claim of the manufacturers of the Digidar that states : "When two vehicles are within the range of the Digidar the speed of the closest vehicle will be indicated." [15,16]. In contrast, the CSIR states that when two or more vehicles are within the range of the instrument it is not known which vehicle's speed is being measured.

Van der Riet further showed that all the other accusations that had been brought against microwave doppler instruments could either be dismissed as having a negligible effect on speed measurement, or could be avoided by careful choice of the speed measurement site [Appendix A].

## 2.4.2 THE VEHICLE IDENTIFICATION PROBLEM

The target identification problem in microwave speed measuring systems arises because of the extreme variation in radar cross section presented by different vehicles. Were the radar cross-section of all vehicles the same, the largest signal would arise from the vehicle closest to the antenna (as the Digidar manufacturers claim), and there would be no identification problem.

Brereton [13] published the results of a test designed to determine the effective radar cross sections of a number of different vehicles. The results of this test are summarised in Table 2.1. All values of radar cross-section are normalised to that of an approaching V. W. Kombi. As can be seen from the Table, the effective radar cross-section of a vehicle is not entirely dependant on the size of the vehicle. The smallest radar cross section does not arise from the smallest vehicle, a motorcycle.

Vehicle	Approaching Radar X-section	Departing Radar X-section
Kenworth Truck	14.58	40.5
Hyno Truck	6.5	3.3
V.W. Kombi	1	1.4
Ford XD Falcon	0.08	1.74
Peugeot 505	0.003	0.09
Leyland Mini	0.1	0.08
Motorcycle (Honda 650)	0.006	0.008

TABLE 2.1 THE EFFECTIVE RADAR CROSS-SECTION OF A NUMBER OF DIFFERENT VEHICLES (NORMALISED TO APPROACHING VW KOMBI)

The highest ratio of radar cross-section occurs between a Kenworth truck and a Peugeot 505. The ratio is 40.5:0.003 or 13500:1. This translates to a 10.8:1 variation in range according to  $r^4$  spreading, where  $r$  is range. Thus a truck 1km away could present a reflected microwave signal equal in strength to a motorcycle merely 100m away from the measuring instrument. In such a case the speed of the truck may be attributed to the motorcycle, possibly resulting in a wrongful prosecution.

The identification problem in conventional instruments is aggravated by the long range performance of these instruments. These instruments are capable of measuring the speed of a vehicle that is not visible to the operator.

It is as a result of the identification problem that "Radar Speed Traps" have fallen into disuse in most parts of South Africa.

## CHAPTER 3 : PROPOSED SYSTEM FOR MICROWAVE SPEED MEASUREMENT

### 3.1 INTRODUCTION TO NEW TECHNIQUE

In this dissertation a new method of measuring vehicle speeds by Microwave Doppler techniques is described. The new technique is aimed specifically at alleviating the problem of vehicle identification associated with conventional instruments.

The proposed arrangement is shown in Figure 3.1. Two microwave sources are used, one with its illumination beam pointing up the road, and the other down. The antennas are arranged in such a way that the illumination beams cross. The complex Doppler signals from both sources are sent to a common signal processing unit where some algorithm is implemented which enables the measurement of the speed of only the vehicle lying inside both illumination beams. Provided that a suitable algorithm can be found, it can be seen that this arrangement could allow the measurement of the speed of a single vehicle in multiple vehicle situations, irrespective of the signal strength of the selected vehicle.

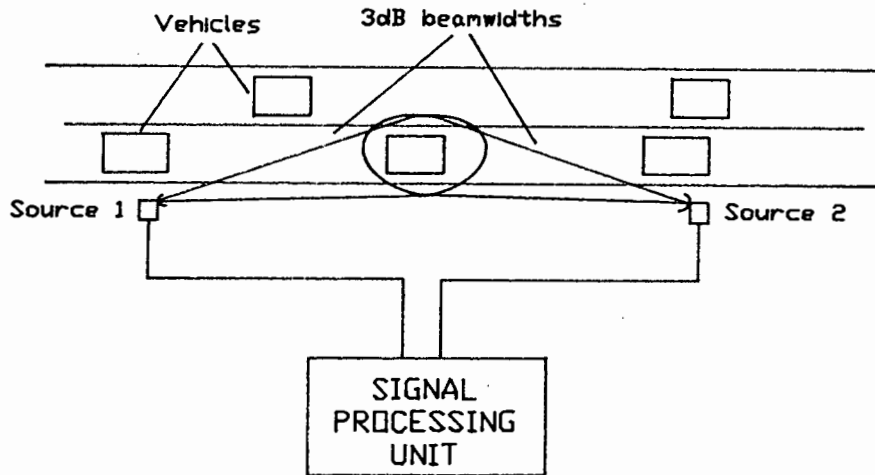


FIGURE 3.1 PROPOSED DOPPLER SPEED MEASUREMENT CONFIGURATION

### 3.2 THE SIGNAL PROCESSING ALGORITHM

In conventional microwave instruments the frequency of the Doppler signal is measured by counting the number of times the signal passes through zero. These instruments, therefore, measure in the time domain. One disadvantage of measuring in the time domain is that in multiple vehicle situations a filter is necessary to ensure that only one frequency (vehicle) is selected. In modern systems this filter takes the form of a phase locked loop (see Figure 2.1). All other dominant frequencies (vehicles) in the bandwidth of interest are ignored.

Figure 3.2 shows the time domain waveform of a complex doppler signal. The recording was made on a freeway with light density traffic. Two vehicles travelling at different speeds were reasonably close to the K-Band microwave transmitter and were contributing most of the doppler

signals present in the complex waveform. For the purposes of this test the signal to noise ratio was considerably degraded by using a low gain antenna of approximately 5dB gain. It can be seen that the signal is fairly noisy. In a conventional speed measuring instrument the phase locked loop would lock onto the highest amplitude sine wave present which has a frequency of approximately 3 KHz. The other vehicle and the noise would be ignored.

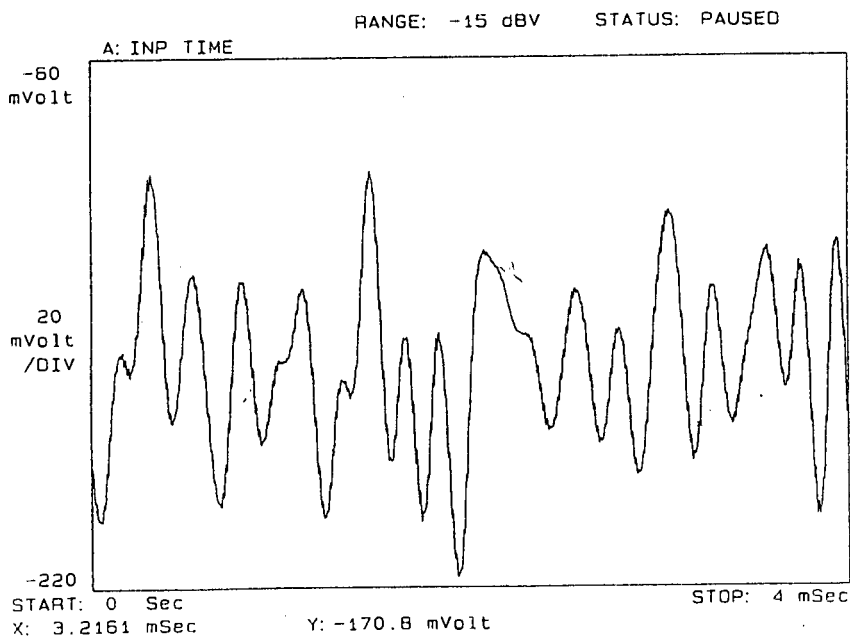


FIGURE 3.2 TIME DOMAIN DOPPLER SIGNAL

If the signal of Figure 3.2 is transformed into the frequency domain, the spectrum shown in Figure 3.3 results. In this case both vehicles are clearly visible as distinct spectral lines. It can be seen that the noise is spread fairly evenly over the bandwidth.

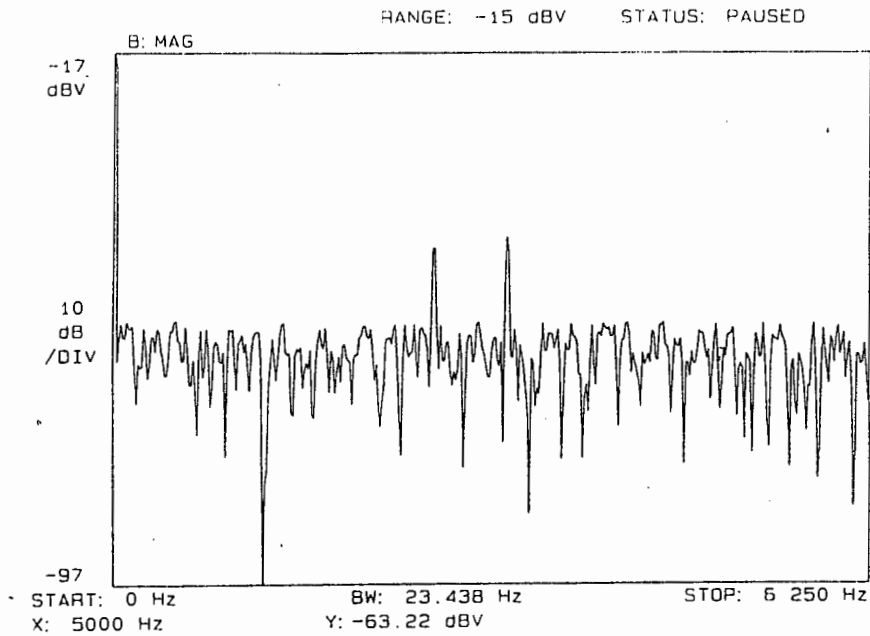


FIGURE 3.3 FREQUENCY DOMAIN WAVEFORM OF THE SIGNAL SHOWN IN  
FIGURE 3.2

The fact that in the frequency domain separate vehicles appear as separate spectral lines can be used to advantage in the arrangement of Figure 3.1. In Figure 3.4 the possible spectra 'seen' by each source are shown. Source 1 'sees' vehicles A, B and C and source 2 'sees' vehicles B and D. Thus vehicle B is the only vehicle seen by both sources. If the spectra of source 1 and source 2 are multiplied together then the desired result is obtained, that is one frequency spectrum containing only the frequency of the vehicle between both sources (vehicle B). Multiplication in the Frequency Domain is equivalent to convolution in the Time Domain, and thus the required algorithm is one of 'Time Domain Convolution.' The algorithm is illustrated in Figure 3.4.

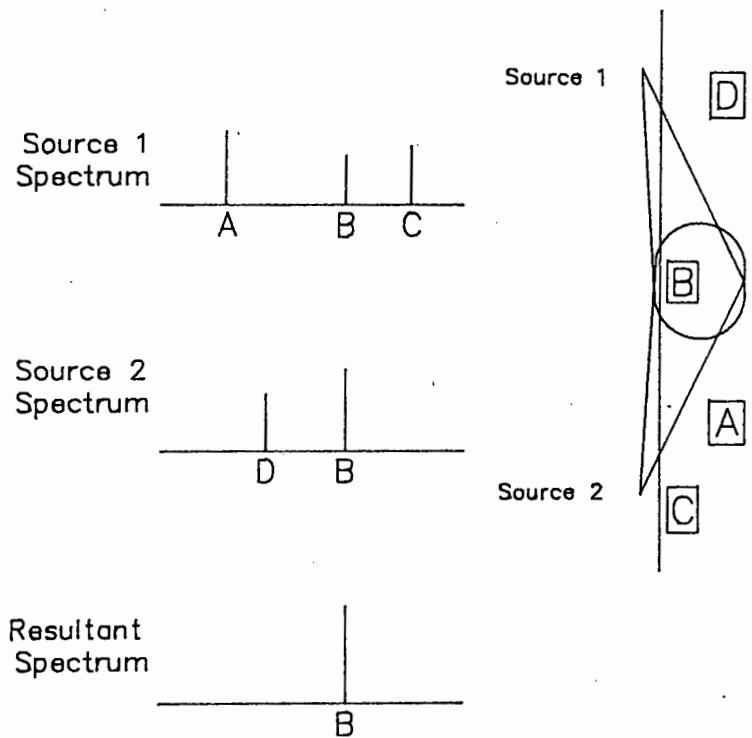


FIGURE 3.4 GRAPHIC REPRESENTATION OF CONVOLUTION ALGORITHM

If the time domain signals originating from the sources are  $a(t)$  and  $b(t)$ , then :

$$R(f) = A(f) \times B(f)$$

$$r(t) = a(t) * b(t)$$

where :  $R(f)$  is the resultant spectrum and is the Fourier Transform of  $r(t)$ ;

$A(f)$  is the Fourier Transform of  $a(t)$

$B(f)$  " " " " "  $b(t)$

and '\*' indicates 'convolution.'

### 3.3 THE CAPTURE AREA

Although the system as described thus far is already an improvement over conventional Doppler Speed Measurement systems, the measurement zone has still not been clearly defined.

It may seem that the measurement zone of the system is defined purely by the intersection of the illumination beams of the two sources. The 3dB contours of the beams illustrated in Figures 3.1 and 3.4 are in reality, however, extremely vague. There is another important factor, caused by the so called 'cosine error', which influences the size of the measurement zone.

Figure 3.5 shows the equivalent road geometry of a conventional microwave speed measurement system. Because vehicles do not travel along the line between the vehicle and the antenna, but rather parallel to the edge of the road, the instrument does not measure the true speed of the vehicle. The resulting measurement error is known as the cosine error, because it is proportional to the cosine of the angle between the road edge and the line joining the source and vehicle. In practice, when a vehicle is a considerable distance from the source, this error is small enough to be neglected.

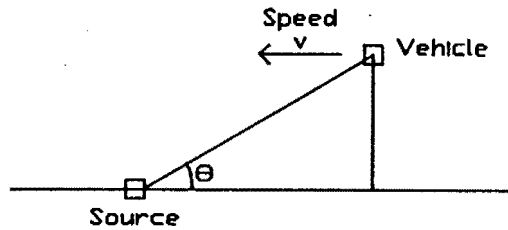


FIGURE 3.5 EQUIVALENT ROAD GEOMETRY OF CONVENTIONAL SPEED MEASUREMENT SYSTEM

With reference to Figure 3.5, the true speed of the vehicle is  $v$ . The measured speed is  $v \cos \theta$ .

Figure 3.6 shows the equivalent road geometry of the proposed system.

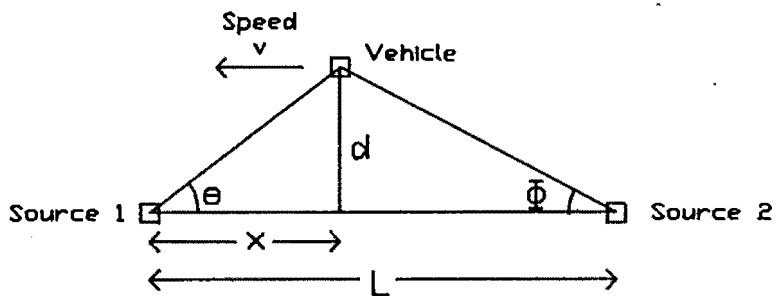


FIGURE 3.6 EQUIVALENT ROAD GEOMETRY OF PROPOSED SYSTEM

Source 1 will read the vehicle speed as  $v \cos \theta$  and source 2 will read the speed as  $v \cos \phi$ . Now, the result of the convolution of  $a(t)$  and  $b(t)$  is zero unless:

$$v \cos \theta = v \cos \phi$$

or :  $\cos \theta = \cos \phi$

or :  $x = L/2$  .

There is of course one exception and that is if  $\theta = \phi = 0$  in which case  $a(t) * b(t)$  is always non-zero. This situation is unlikely, however, to occur in practice.

The resolution of the system shall be defined as the maximum difference between the speeds seen by sources 1 and 2 for which the convolution is non-zero. The resolution shall be denoted  $r$  and have units of km/h. If the resolution is infinitely high then  $r=0$  and the convolution is non-zero only at  $x = L/2$  or  $\theta=0$ , as previously shown. For  $r$  not equal to zero, there is an entire area for which the convolution is non-zero. This area shall be known as the 'capture area'.

The equation defining the boundary line of the capture area can be found from simple geometry. On the 'Source 1' side of the area, the boundary line is defined by the equation:

$$v \{ \cos \tan^{-1}(d/x) - \cos \tan^{-1}(d/L-x) \} + r = 0$$

where  $s$  : speed (km/h)  
 $d$  : Distance of vehicle from base line (m)  
 $x$  : Distance of vehicle from Source 1  
 $L$  : Distance between Source 1 and Source 2  
 $r$  : resolution (km/h)

The Capture Area is illustrated in Figure 3.7 for vehicles travelling at 100km/h, a distance  $L$  between the Sources of 70m, and a resolution of 1km/h.

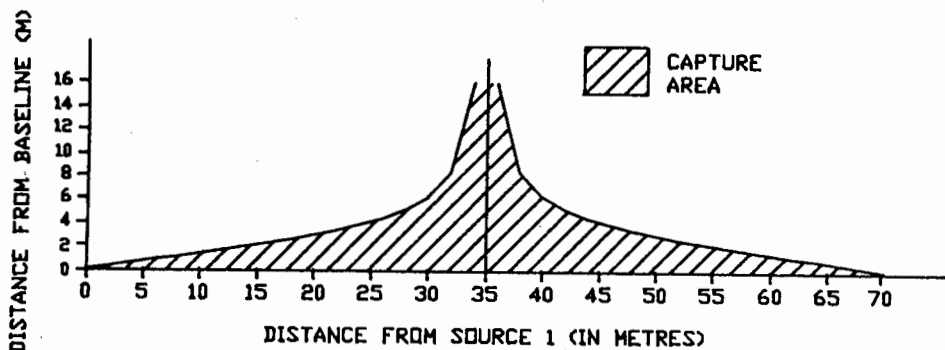


FIGURE 3.7 CAPTURE AREA (S=100M, L=70M, R=1KM/H)

The Capture Area is symmetrical about the  $x=L/2$  line.

If omni-directional antennas were used, the capture area would extend beyond the limits shown in Figure 3.7. Parts of the Capture Area would exist where  $x < 0$  and  $x > L$  and the area would be symmetrical about the  $d=0$  line.

The choice of  $L$  depends not only on the size of the capture area desired but also on the maximum cosine error that can be tolerated. Figure 3.8 shows the percentage error in speed incurred against the vehicle distance from the baseline,  $d$ , for various values of  $L$ . It would seem desirable to make  $L$  as large as possible but this would be at the cost of reduced target discrimination as the chance of more than one vehicle entering the capture area at one time is then much higher.

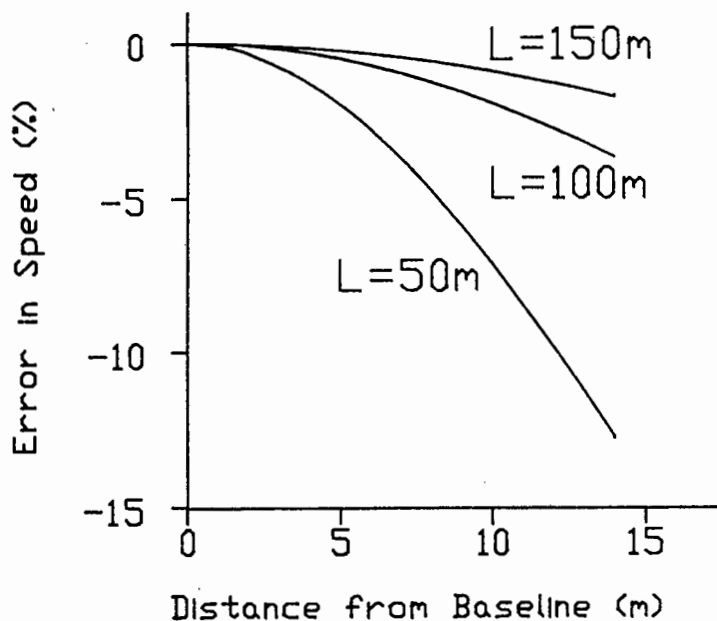


FIGURE 3.8 SPEED ERROR DUE TO COSINE ANGLE FOR VARIOUS  
VALUES OF L

The measurement zone is now much more clearly defined than it was by the illumination beams alone. In practice there are a number of other factors which influence the size and shape of the measurement zone, although none have as much effect as the cosine error. These other factors are discussed in Section 8.3.1.

## CHAPTER 4 PRACTICAL IMPLEMENTATION

### 4.1 INTRODUCTION

A detailed study of the individual components of the practical microwave speed measurement system is given in chapters 5,6 and 7. It is the purpose of this chapter to provide a brief overview of the complete practical system.

### 4.2 SYSTEM OVERVIEW

It can be seen from the diagram of the proposed system (Figure 3.1) that the complete system can be divided into three main component parts :

- (i) The Microwave Sources,
- (ii) The Signal Processor.
- (iii) The Interface between the Signal Processor and Microwave Sources.

The system components are shown in Figure 4.1.

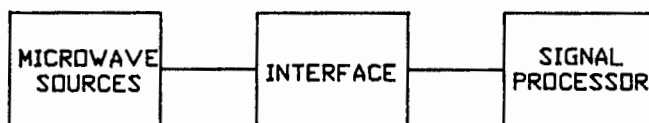


FIGURE 4.1 SPEED MEASURING INSTRUMENT SYSTEM COMPONENTS

Of these components, the Signal Processor is the most complex. This aspect of the system will be discussed first.

### 4.3 SIGNAL PROCESSOR

#### 4.3.1 SIGNAL PROCESSING CONSIDERATIONS

The signal processing requirements of the proposed speed measurement system are complex. The choice of a suitable signal processor was, therefore, an important one. In making this choice the following all had to be considered:

- i) Complexity: The processor had to be able to handle the complexity of the computation, in particular the convolution algorithm.
- ii) Speed: Speed measurements must be made virtually in real time. The processor therefore has to perform the computation quickly.
- iii) Flexibility: It was envisaged that a number of changes to the system would be made before an optimum solution would be found. With this in mind, one of the requirements of the signal processor was that it be adaptable.
- iv) Cost: Although this factor is not as important as the ones mentioned above, the relative cost of the signal processing circuitry should not be too high.

The first decision that had to be made was whether an analog or a digital processor was to be used.

An Analog Processor has the advantage of speed but may not be able to handle the complexity of the computation. Convolution is a fairly complicated task to perform by analog means as some method of storing signal levels must be provided. In conventional Analog convolvers, discrete signal levels are stored in so-called 'bucket-brigade' devices. A further disadvantage of Analog Processors is that they are totally dedicated to the task they are designed for and thus do not offer flexibility.

A digital, or microprocessor-based signal processor looked more attractive, as it could meet both the complexity and the flexibility requirements, but not necessarily the speed requirement.

#### **4.3.2 THE DEVELOPMENT OF DEDICATED DIGITAL SIGNAL PROCESSORS**

General purpose microprocessors, are not, in general, suitable for Digital Signal Processing (DSP) applications. This is primarily because of the problem of processing speed. Real time processing is normally limited in general-purpose microprocessors to signal frequencies not in excess of 1 KHz. This has restricted the use of these processors for DSP applications to the industrial field where the sampling rate is commonly in the range 1 Hz to 1 KHz [17].

The first dedicated DSP chip, the Intel 2920, appeared on the market in 1980 [18]. This processor features fast, on-board program memory, fast data memory, A/D and D/A converters. Since then a large number of DSP chips have been introduced, with increasing complexity.

The TMS32010, introduced in 1983, was the 3rd DSP chip to appear. This signal processor was one of the 'second generation' of DSP chips. The TMS32010 differed from other processors in that it contained an on-board hardware

multiplier and shifter [19]. Thus it is possible with the TMS32010 to perform multiplication, one of the most common DSP operations, in a single clock cycle. It was primarily because of this feature that the TMS32010 rapidly became well established in the field of Digital Signal Processing.

At the time of writing the cost of this processor is approximately R100.

It can be seen that this processor meets the requirements of flexibility, speed, cost and complexity, and it is on the TMS32010 that the signal processing of the prototype speed measuring instrument is based.

The data sheet for the TMS32010 is included in Appendix D. The Signal Processing Hardware and Software is discussed in detail in Chapter 7.

## 4.4 MICROWAVE SOURCES

### 4.4.1 FREQUENCY

The first decision to be made in the selection or design of a Microwave Source for the instrument, is that of the frequency of operation. In Doppler Speed Measuring Instruments the operating frequency is constrained by :

- (i) The Time to make a speed measurement; and
- (ii) The Physical size of the microwave components.

If the operating frequency is too low, the resulting doppler signals are also low in frequency. It thus takes much longer to make a speed measurement with a certain frequency

resolution than it would if a higher transmit frequency was used. Another disadvantage of a low operating frequency is that the physical size of the Microwave equipment, in particular the antenna, is much larger than for a higher frequency. (In 'police radar' it is advantageous to keep the microwave sources and antenna as small as possible so that they are not easily seen by passing motorists.)

The constraint on the upper frequency limit for the Microwave Source is simply the high cost of Microwave components at these frequencies.

The frequency band of 24.10 to 24.20 was chosen for the microwave sources used in the instrument. This band is a compromise between the larger size of the equipment at lower frequency bands and the greater cost of Microwave devices at higher frequencies.

#### **4.4.2 RANGE, ANTENNA GAIN, POWER AND SENSITIVITY**

One disadvantage cited with conventional Doppler Speed Measuring Instruments is their long range performance [14]. In the proposed system the measurement zone is well defined and a long operating range is unnecessary and even undesirable. Although the optimum range is still to be found, a range of 100m for each source for a 'standard' car was considered a conservative estimate for the maximum range necessary for the instrument. It is thus possible to tolerate lower antenna gain, lower transmit power and lower receiver sensitivity than in the Microwave sources for conventional instruments.

The design and construction of a Microwave Source for the speed measuring instrument is discussed in detail in Chapter 5.

## 4.5 INTERFACING CIRCUITRY

### 4.5.1 INTRODUCTION

In order to interface the Analog signals from the Microwave sources to the TMS32010 microprocessor a certain amount of interfacing circuitry is necessary.

The most obvious function of the interface is to perform the Analog-to-Digital (A/D) conversion in order to convert the analog doppler signals into a form 'readable' by the digital processor. The conversion rate of the A/D converter must be accurately known in order to accurately measure vehicle speeds.

### 4.5.2 DYNAMIC RANGE

An important function of the interfacing circuitry is that of extending the dynamic range of the instrument by means of an Automatic Gain Control (AGC) amplifier. If an AGC amplifier were not included, the dynamic range of the instrument would be limited by the effective dynamic range of the Signal Processor, which in turn is a function of the number of bits in the A/D converter.

The dynamic range of the instrument was chosen to be 110dB. A high operating dynamic range ensures that the instrument can operate with a wide range of vehicle radar cross-sections. The dynamic range in this instrument is equal to the sum of the dynamic range of the A/D converter and that of the AGC.

The dynamic range will be divided up as:

A/D converter : 50dB

AGC amplifier : 60dB

A detailed description of the Interfacing Circuitry for the instrument can be found in Chapter 6.

## CHAPTER 5 : SOURCE

### 5.1 MICROWAVE OSCILLATORS

#### 5.1.1 INTRODUCTION

Solid state microwave oscillators first became commercially available after the discovery of the so-called 'Gunn Effect' in Gallium Arsenide (GaAs) [20,21]. Up until that time the only means of generating low to medium power at microwave frequencies was with klystrons. As with other vacuum tube devices, klystrons require high voltage power supplies that are difficult to generate with batteries; thus restricting their use in portable equipment.

The Gunn Effect diode is a two-terminal negative resistance device. An oscillator is formed by applying the correct bias to the Gunn diode and mounting the diode in parallel with a resonant circuit. When used in the delayed domain mode [22], the oscillator can be tuned by modifying the centre frequency of the resonant circuit. In a practical Gunn oscillator the resonant circuit is formed by a combination of the package housing the GaAs slice, the mounting posts and the parameters of the cavity. The optimum working frequency of a particular Gunn diode is determined primarily by the thickness of the GaAs slice.

Since the introduction of Gunn Diodes, other microwave solid-state active devices have become commercially available, the most important of which are Gallium Arsenide Field Effect Transistors (GaAs FET's). GaAs FET's, being three-terminal devices, are most suitable for planar circuits, that is, layout on a suitable microwave substrate. The most popular microwave substrate currently available,

microstrip, becomes unusable at frequencies much above 20GHz due to losses in the dielectric material. The selected frequency of operation for the prototype instrument, 24GHz, prohibited the use of microstrip oscillators and thus only cavity (waveguide) oscillators were considered. Gunn diodes were selected as the active microwave devices in the cavity oscillators because of the difficulty of mounting FET's in three-dimensional structures.

### 5.1.2 CAVITY GUNN OSCILLATORS

Microwave propagation through waveguide occurs with very low loss. This means that it is possible to form low loss (high Q) resonant cavities in waveguide which can be used as the external circuit for microwave oscillators. High Q resonant circuits are important if low noise and good frequency-temperature characteristics are required.

The cross-sectional view through a typical cavity Gunn oscillator is shown in Fig 5.1. The adjustable short circuit allows mechanical tuning of the oscillator. A large tuning range is possible [23]. The matching post is necessary to match the device impedance to that of the waveguide. The effects of the adjustable short circuit and the matching post are not independent and care must be taken in the design of these components.

Bias to the device is provided through a microwave choke. In Fig 5.1 a three-section choke is shown. The choke consists of a low impedance section, a high impedance section and finally another low impedance section. Each section is  $\lambda/4$  long, where  $\lambda$  is the wavelength.

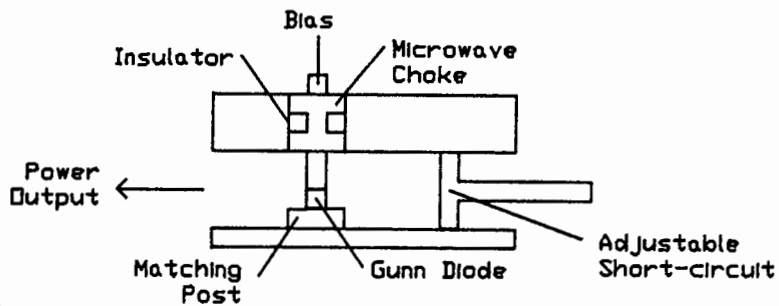


FIGURE 5.1 CROSS-SECTION THROUGH TYPICAL CAVITY GUNN OSCILLATOR

## 5.2 PROTOTYPE OSCILLATOR

### 5.2.1 GUNN DIODE CHARACTERISTICS

Commercially available microwave oscillator and mixer combinations are expensive. For this reason the sources used in the microwave speed measuring instrument were 'custom built'.

In the prototype microwave sources, devices intended for 'burglar alarm type' applications were used. The system requirements of low power and low cost make these devices an ideal choice for the speed measuring instrument.

The characteristics of the Gunn diode that was selected are:

MANUFACTURER : MICROWAVE ASSOCIATES  
PART NUMBER : MA49628  
CENTRE FREQUENCY : 24.1 GHz  
OPERATING VOLTAGE : 5.0V  
OPERATING CURRENT : < 200mA  
POWER OUTPUT : > 10mW

### 5.2.2 OSCILLATOR DESIGN

The design of the prototype oscillator was based on the oscillator illustrated in Figure 5.1. The engineering drawings for the manufacture of the sources are given in Appendix B.

The 'Y-Z plane' cavity dimensions of the oscillator were made the same as K-band waveguide. This had the advantage that standard connectors (such as co-axial to waveguide transformers) could be used in making the measurements of power output and frequency. The position of the terminating short circuit at the rear of the cavity could be adjusted by inserting spacers of varying thickness between the short circuit and the cavity. Fine tuning of the oscillator frequency was provided by a lockable screw protruding into the cavity.

The optimum distance between the device and the short circuit was found by experimentation to be  $0.181\lambda$ . The optimum size matching post was found to be 7mm in diameter and 1mm thick. Two oscillators were constructed and their respective power outputs are:

SOURCE 1 : 12.5 mW  
SOURCE 2 : 11.3 mW

## 5.3 MICROWAVE MIXERS

### 5.3.1 SELF MIXING OSCILLATORS

The self-mixing oscillator (SMO), or self-oscillating mixer was proposed in 1971 [25,26]. Receiver systems incorporating SMO's have the advantage that no external mixer is required. The conventional biasing arrangement for a Gunn Diode SMO is shown in Figure 5.2.

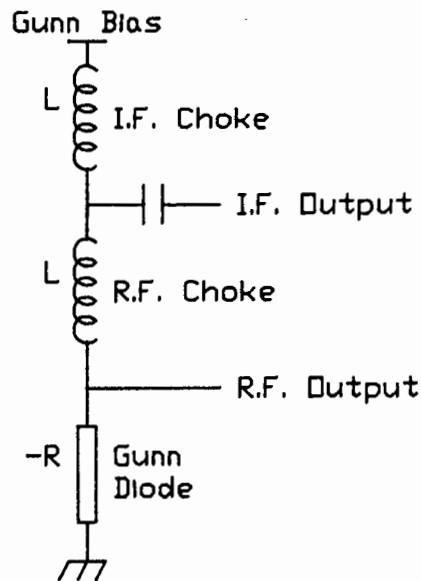


FIGURE 5.2 BIASING ARRANGEMENT FOR GUNN DIODE SELF-MIXING OSCILLATOR

The maximum attainable Noise Figure of the SMO arrangement is typically 10dB worse than the separate oscillator and mixer counterpart.

The SMO is particularly suited to systems where the I.F. is high in frequency, as the I.F. choke is then simple to construct. In the proposed system the minimum I.F. (doppler) frequency is approximately 300Hz. It is not easy to construct an effective I.F. choke at this frequency.

For this reason an external mixer diode was used in the system.

### **5.3.2 MIXER DIODES**

Mixer diodes convert radio frequency energy (RF) to an intermediate frequency (IF). In essence a mixer diode operates as a very fast switch. The switching speed is controlled by a local oscillator (LO) whose amplitude is substantially greater than that of the RF signal. The IF is then the difference between the LO and RF frequencies.

In converting from RF to IF there is an associated conversion efficiency. This conversion efficiency is an important factor that must be considered when designing a mixer, as a high conversion loss results in a high noise figure [24]. The conversion loss is a function of the mixer diode itself and the bias applied to it. Conversion loss is discussed in section 5.6.2.

## **5.4 PROTOTYPE MIXER**

### **5.4.1 MIXER DIODE CHARACTERISTICS**

The device chosen for use in the prototype instrument is, as with the Gunn Diode, one that is intended for burglar alarm type applications. This mixer diode has a relatively high noise figure and a low conversion efficiency. The resulting signal to noise ratio is, however, sufficiently high for use in the prototype speed measuring instrument. The mixer diode specifications are:

MANUFACTURER : MICROWAVE ASSOCIATES

PART NUMBER : MA4E735

OPERATING FREQUENCY : 24 GHz

NOISE FIGURE : approx. 10dB.

#### 5.4.2 MIXER DESIGN

The design of a mixer mount is in general a non-trivial problem. Some means must be provided for coupling both RF and LO power into the mixer diode. Where microwave sources are to be used as doppler sensors, the problem is made more difficult by the fact that the LO power must not only be fed to the mixer, but also transmitted. This requires a power divider somewhere in the source.

A simple although inefficient means of coupling both RF and LO power into the mixer diode is to mount the diode directly in front of the oscillator. This is the technique employed in the prototype instrument.

The greatest disadvantage of this method of mounting the mixer is that the coupling between the mixer and local oscillator is extremely high and thus 'wastes' LO power. In the proposed speed measuring instrument, however, where short range and low power are desirable, tight coupling can be tolerated. The LO power not absorbed leaks past the mixer diode to be transmitted. The reflected signal returns through the antenna and is fed directly to the mixer. This arrangement is shown in Figure 5.3.

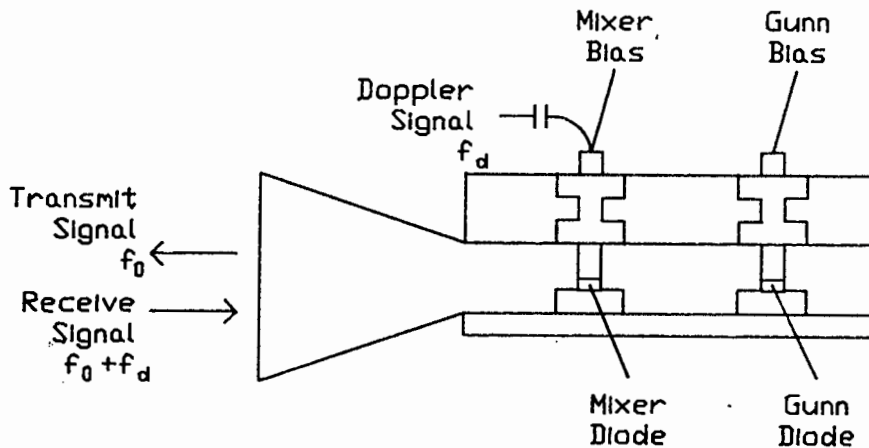


FIGURE 5.3 GUNN OSCILLATOR AND MIXER COUPLING TECHNIQUE

There are, in fact, two advantages to be gained from the mixer mounting technique just described:

(i) It provides some isolation between the oscillator and the antenna. If there were no isolation large vehicles close to the oscillator could 'pull' the oscillator frequency, causing speed measurement errors. Because isolation is provided in part by the mixer, no separate mixer is required.

(ii) Up to some optimum operating point, the noise figure (NF) of the mixer decreases as the local oscillator power into the mixer increases. This must of course be seen in the light of the loss of transmitter power.

The cavity that was designed for the oscillator was also used for the mixer (see Appendix B). The spacers used to determine the optimum distance between the Gunn diode and short circuit were used to find the optimum distance between the Gunn and Mixer diodes. This distance was found to be  $0.45\lambda$ . Two mixer units were built.

### 5.4.3 OSCILLATOR AND MIXER COUPLING

When the mixers were placed in front of the oscillator sections the measured output powers were:

SOURCE 1 : 2.5mW

SOURCE 2 : 2.2 mW

It can be seen that approximately 80% of the power provided by the local oscillator is 'absorbed' by the mixer.

The coupling factor,  $\beta$ , can be defined for this configuration as:

$$\beta = \frac{\text{Power dissipated in the Mixer}}{\text{Transmitted Power}}$$

In the conventional definition of  $\beta$ , critical coupling between two devices occurs when the power dissipated in each device is the same. When  $\beta < 1$  the system is under-coupled and when  $\beta > 1$  the system is over-coupled. Thus in this system critical coupling occurs when the power dissipated in the mixer equals the transmitted power.

$$\text{Here } \beta \approx \frac{(12.5-2.5)}{2.4} \quad [\text{for Source 1}]$$

$$\text{Thus } \beta = 4 \quad (\text{over-coupled}).$$

## 5.5 BIAS

### 5.5.1 GUNN OSCILLATOR BIAS

The Gunn diode requires a bias of 5V with a maximum current of 200mA. The 5V supply must be stable as the frequency of operation is partly dependant on the supply voltage. The

supply must also have a low ripple content as any supply ripple results in undesirable F.M. noise (see Section 5.6.1). The bias for the Gunn diode is shown in Figure 5.4 together with protection circuitry for the device in the event of a power supply fault.

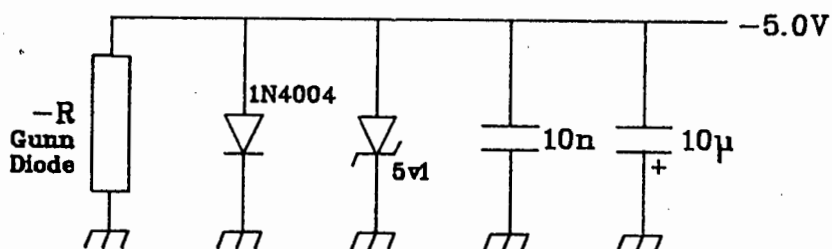


FIGURE 5.4 GUNN OSCILLATOR BIAS CIRCUIT

### 5.5.2 MIXER BIAS

The mixer diode rectifies the local oscillator current that is generated across it, thus forming a d.c. current in the diode. This current requires a d.c. path and this is usually provided by a resistor between the mixer and ground. Such an arrangement is known as self-biasing, as the current through the mixer diode generates a voltage across the diode which biases it at some point in its characteristic. The value of the resistor must be chosen carefully for minimum conversion loss and maximum signal to noise (S/N) ratio. In the prototype sources the optimum value of resistor was found to be  $470\Omega$ . The biasing arrangement for the mixer is shown in Figure 5.5.

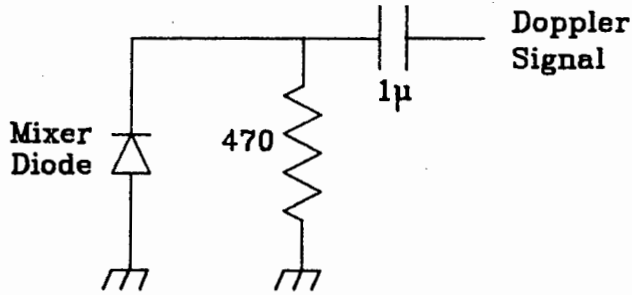


FIGURE 5.5 MIXER DIODE BIAS CIRCUIT

## 5.6 NOISE CONSIDERATIONS

### 5.6.1 OSCILLATOR NOISE

Virtually all noise in Gunn oscillators manifests itself as phase noise. There are three main sources of phase noise in Gunn oscillators [27]:

(i) Flicker noise : This noise is active at frequencies less than 10kHz away from the carrier. This noise is common to most active devices and has a  $1/f$  spectrum.

(ii) Recombination noise : This noise is a function of the semiconductor material. It also follows a  $1/f$  spectrum, is temperature dependant and active at frequencies less than 20MHz away from the carrier.

(iii) Noise generated at the RF frequency (not FM noise). This is analogous to shot noise.

Both flicker noise and recombination noise are filtered by the effective (loaded)  $Q$  of the resonant circuit. Thus a

high Q external resonant circuit will greatly reduce the FM noise of the oscillator.

Figure 5.6 shows the spectral purity of the oscillator over a 2MHz span. This measurement was made on an HP70000 Spectrum Analyser. It can be seen that the oscillator is extremely noisy, especially at frequencies closer than 10KHz to the baseband where all the doppler frequency measurements are made [see Section 5.9]. Much of this noise can be attributed to the poor quality of the Gunn Diode.

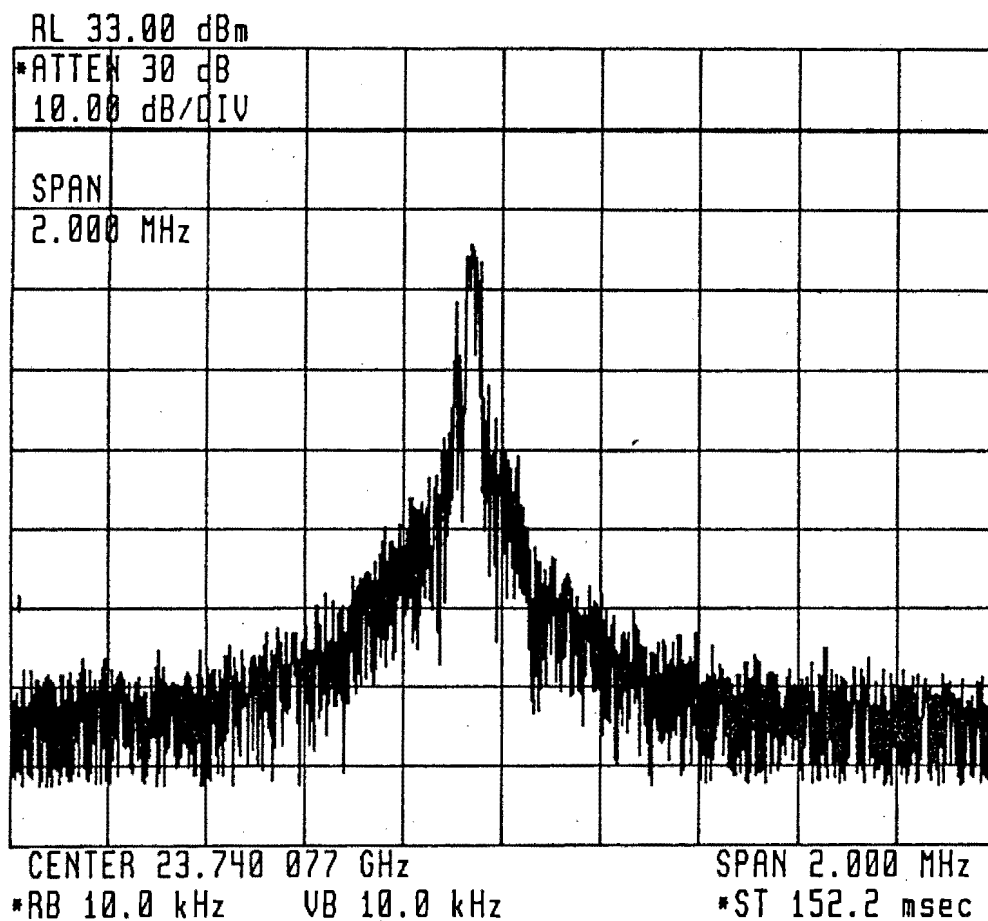


FIGURE 5.6 GUNN OSCILLATOR NOISE

In conventional heterodyne systems employing mixers, the maximum attainable signal to noise ratio at the IF is

restricted by the level of noise present in the local oscillator the IF distance away from the carrier. If this held true for this system, where the IF is low in frequency and the local oscillator noise high, the system dynamic range would be so low as to render the system virtually unusable. It has been shown [28], however, that in Doppler systems where the delay between the transmit and receive signals is small, the decorrelation between the transmitted noise and received noise is very small. This is explained by modelling the noisy local oscillator as a noise-free oscillator which is frequency modulated by a random, low frequency signal. Provided that the time delay is short, the received doppler signal will mix with a local oscillator of almost exactly the same frequency and phase that was transmitted. If taken to the limit, this means that it is possible to transmit an arbitrarily noisy signal with no consequent degradation to the signal to noise ratio of the doppler signal. The limiting factor is the speed resolution desired. In the proposed system, where a speed resolution of 0.5% is adequate and the delay is small due to the short range operation, local oscillator noise less than 50MHz from the carrier will degrade neither the doppler S/N ratio or the speed resolution.

### **5.6.2 MIXER NOISE**

There are a large number of factors contributing to the addition of unwanted noise to the signal at the IF output of the mixer. The most important of these are:

(i) Image noise : In the mixing process both the signal and its image are converted to the image frequency. While there is no signal at the image frequency, there is noise present. This effectively doubles the noise power, resulting in a degradation of the S/N ratio by 3dB.

(ii) Diode thermal noise : This is the bulk of the noise generated by the diode itself and is caused by parasitic resistance in the diode. This noise is temperature dependant.

(iii) Excess noise : This is junction noise which becomes serious particularly at low modulation frequencies (close to baseband). This noise has a  $1/f$  spectrum.

(iv) LO noise : Again this noise is a serious problem at low frequencies. The noise sidebands of the local oscillator overlap the signal at the IF frequency. This LO sideband noise also has a  $1/f$  spectrum.

(v) IF noise : This is noise added by the IF amplifier.

In doppler speed measuring instruments that operate at baseband the 'IF' signals occur at very low frequencies; in the proposed instrument they lie in the audio band [see Section 5.9]. It has been shown that LO noise in this system will not significantly affect the noise in the doppler signal so that Excess noise will be the major contributing factor to the total noise content.

In cases where the mixer is driven hard, as in this source, the noise contributed by the image and the diode thermal noise almost exactly make up for the noise lost in making the conversion [24]. The signal power is obviously not regained so that the decrease in signal to noise ratio during conversion is approximately equal to the conversion loss.

The noise figure of the mixer can now be expressed as :

$$NF = L_C + N_E + N_{IF}$$

where

NF : noise figure  
L<sub>C</sub> : conversion loss  
N<sub>E</sub> : excess noise  
N<sub>IF</sub> : IF amplifier noise

There are of course other factors contributing to the total noise present but they are insignificant in comparison to those already discussed.

## 5.7 ANTENNA

### 5.7.1 INTRODUCTION

The choice of a suitable antenna is important as it affects both the size of the measurement zone and the signal to noise ratio. The requirements of the antenna are:

- (i) Physically small size to reduce visibility
- (ii) Sufficient Gain
- (iii) Low sidelobe levels.

At a frequency of 24 GHz only two types of antenna are practical :

- (i) Horn Antennas
- (ii) Parabolic Prime-Focus fed Antennas or Cassegrains

In cases where high gain and narrow beamwidths are required, parabolic antennas are more attractive than horns because of

their smaller volume. Conventional microwave speed measuring instruments all use high gain Cassegrains.

For the prototype instrument horn antennas were chosen. Horn Antennas are more attractive where low gains and wider beamwidths can be tolerated, resulting in a smaller antenna. In such situations parabolics are not suitable as it is not practical to feed a parabolic antenna with an aperture size of less than about 8 wavelengths. Horns are also simpler to construct than parabolic antennas, needing no feeds or subreflectors.

### 5.7.2 ANTENNA GAIN

At first it may seem advantageous to make the antenna gain as high as possible. This would result in a higher signal level (and thus higher S/N ratio) and a narrow beamwidth which would aid in defining the measurement zone. However, Andersen [29] has shown that it is unwise to use a narrow beamwidth when measuring vehicle speeds by microwave means.

The Doppler spectrum is the product of the Antenna spectrum and the Object Spectrum. Andersen represents this relationship as :

$$B(w) = G(w) F(w)$$
$$\text{or } b(t) = g(t) * f(t)$$

where  $B(w)$  : Doppler Spectrum  
 $G(w)$  : Antenna Spectrum  
 $F(w)$  : Object Spectrum

and  $b(t)$ ,  $g(t)$  and  $f(t)$  are the Inverse Fourier Transforms (IFT's) of  $B(w)$ ,  $G(w)$  and  $F(w)$  respectively.

Thus in order to measure true radial speed the ideal situation would be a moving point reflector illuminated by an omni-directional antenna. A point reflector has a constant phase centre and in this case  $B(w)$  would be a single, infinitely narrow spectral line.

If a narrow beamwidth illuminates a large vehicle there is a moving phase centre across the vehicle. This has the effect of frequency modulating the doppler spectrum which results in spectral 'smearing'. In the proposed system such smearing is undesirable as it would cause the convolution of the signals from the two sources to be non-zero for a range of frequencies (viz. speeds). A 'smeared' spectral line can also be interpreted as a clean spectral line with added F.M. noise, and thus the S/N ratio of the system is degraded.

Figure 5.7 shows a comparison between the measured frequency (doppler) spectra from a vehicle when two different antennas were used. One antenna had a gain of 8dB and the other a gain of 22dB. Spectral smearing is evident from the 22dB gain antenna. These signals were recorded at the roadside on a portable tape recorder and later analysed in the laboratory with an HP3561A Dynamic Signal Analyser.

It is interesting to note that when vehicles pass very close to the antenna, spectral smearing due to moving phase centres is inevitable, even if omni-directional antennas are used. The effects of spectral smearing on speed measurement is discussed in Section 8.3.2.

### 5.7.3 HORN ANTENNA DESIGN

For the prototype instrument two antennas of different gains were constructed. This allowed a comparison to be made between the effect of a 'high' gain antenna of 22dB and a 'medium' gain antenna of 8dB.

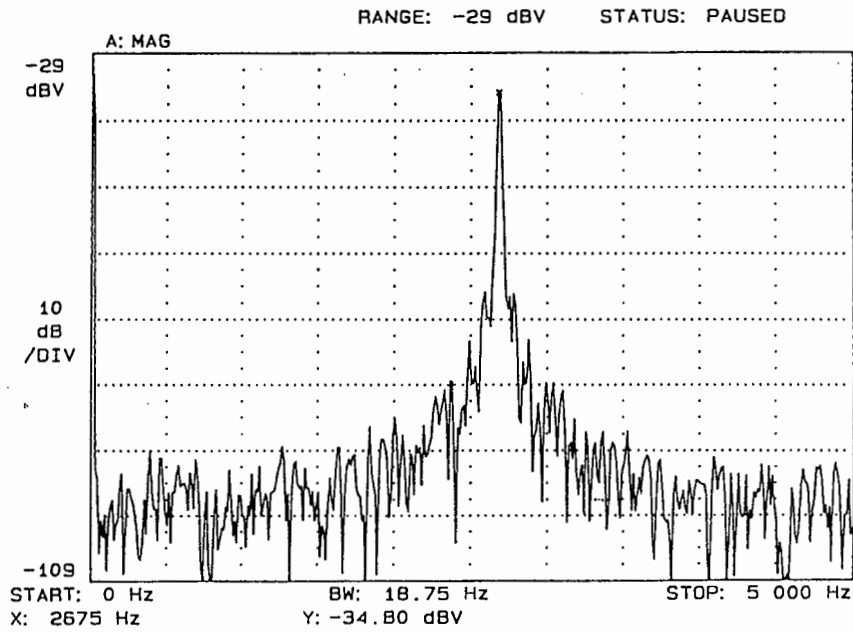


FIGURE 5.7A DOPPLER SPECTRUM FROM SINGLE VEHICLE  
(8dB GAIN ANTENNA)

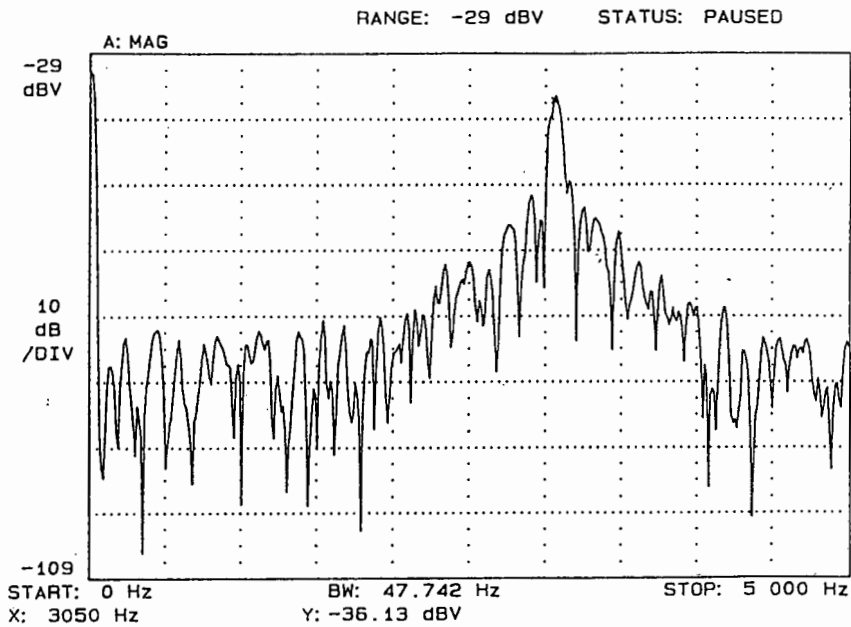


FIGURE 5.7B DOPPLER SPECTRUM FROM SINGLE VEHICLE  
(22dB GAIN ANTENNA)

In a horn antenna the antenna gain is given by:

$$g = \frac{4\pi ab\eta}{\lambda^2}$$

where

$\eta$  : efficiency of the antenna

a,b : dimensions of the horn aperture

$\lambda$  : waveguide wavelength

The efficiency of a Horn Antenna is very high and thus is often approximated as 1.

The critical factor in the design of a horn antenna is the flare of the antenna. If the flare is too 'sudden' then the phase of the signal at the edge of the horn lags that of the centre. If the phase lag is considerable then the antenna efficiency drops and large sidelobes are produced. The ideal flare is one which is very gradual, but this results in a very long antenna, and so a compromise must be reached. The maximum permissible phase lag for a 'good' horn antenna with high efficiency and low sidelobe levels is  $\lambda/6$ .

The construction drawings for the antennas are given in Appendix B. The prototype horns were manufactured from sheets of brass soldered together.

## 5.8 OSCILLATOR FREQUENCIES

In order for the two microwave sources not to interfere with each other, it was necessary to offset their frequencies. Interference would occur if the frequencies came within approximately 12kHz of each other - the doppler bandwidth of the instrument [see Section 5.9].

Using the tuning screws mounted at the rear of the oscillator cavities, the frequencies of the sources were adjusted to the values given shown below. The sources were offset 50MHz from each other at a temperature of 20°C. Although this margin may seem unnecessarily large, differences in temperature between the sources could cause their frequencies to approach each other. Figure 5.8 shows a graph of the source frequencies plotted against temperature. It can be seen that there is a possibility of interference between the sources if their temperatures differ by more than 20°C. This was considered a realistic figure for cases where one source was placed in the sun and the other in the shade.

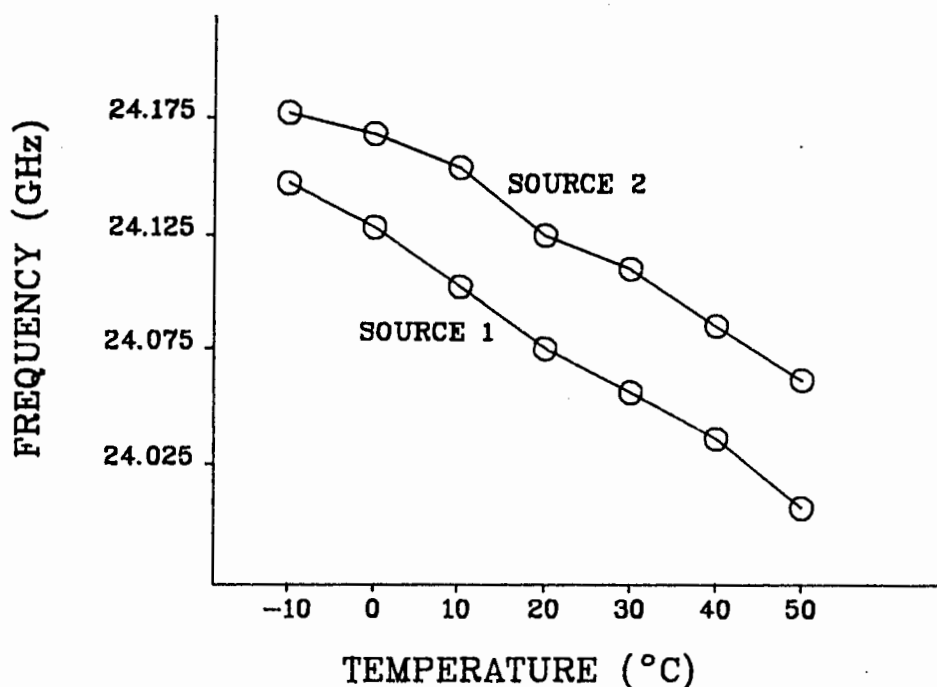


FIGURE 5.8 SOURCE FREQUENCIES VERSUS TEMPERATURE

An HP5351B MICROWAVE FREQUENCY COUNTER was used to measure the frequencies.

## 5.9 DOPPLER FREQUENCIES

The resultant Doppler frequencies from the two sources for vehicles travelling at various speeds are shown below. There is only a 0.2% difference in Doppler frequency 'seen' by the sources and thus no compensation for frequency is necessary.

The doppler frequency for a vehicle travelling at 256 km/h is given as it is used to determine the sampling rate of the A/D converter [see Section 7.4.2.2].

Vehicle Speed (km/h)	Doppler Frequency Source 1 (kHz)	Doppler Frequency Source 2 (kHz)
50	2.229	2.234
100	4.459	4.468
150	6.688	6.702
200	8.917	8.936
256	11.413	11.437

TABLE 5.1 DOPPLER FREQUENCIES 'SEEN' BY BOTH SOURCES

From these values it can be seen that the 'doppler bandwidth' of the instrument is approximately 12kHz.

## CHAPTER 6 : INTERFACING CIRCUITRY

### 6.1 INTERFACING CONSIDERATIONS

#### 6.1.1 INTRODUCTION

It is the purpose of this chapter to describe the circuitry which interfaces the low level doppler signals from the mixers of the two sources to the microprocessor. The speed readout, or display, is also discussed in this chapter. The following aspects of the system are dealt with:

- (i) Low noise pre-amplifier for the doppler signals,
- (ii) Cable (for transferring the doppler signals from the Source to the processor),
- (iii) Automatic Gain Control (AGC) circuitry,
- (iv) Multiplexor and Anti-aliasing Filter,
- (v) Analog to digital converter,
- (vi) Display.

A block diagram of the interfacing circuitry is shown in Figure 6.1.

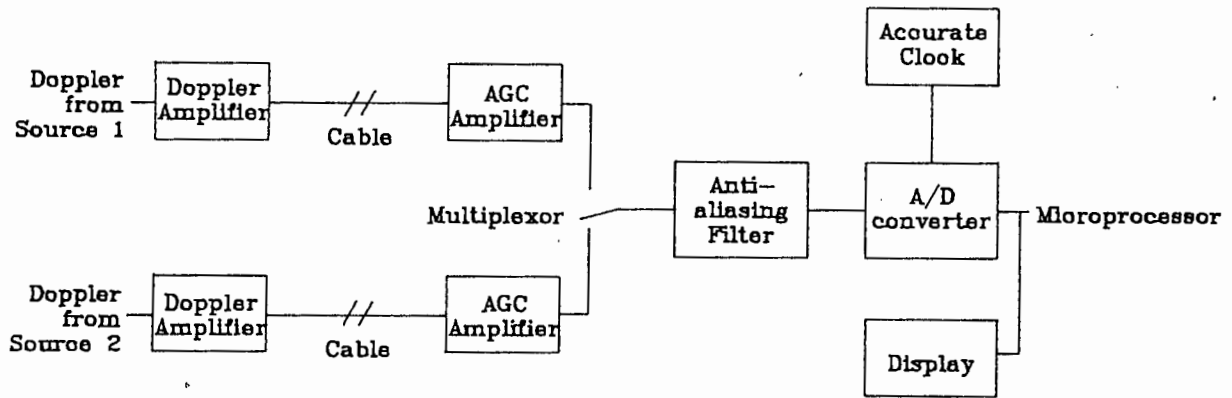


FIGURE 6.1 BLOCK DIAGRAM OF INTERFACING CIRCUITRY

The inputs to the interfacing circuitry are the low level doppler signals. The outputs are the microprocessor communication lines which must still be defined before the interfacing circuitry can be designed.

#### 6.1.2 TMS32010 COMMUNICATION LINES

The TMS32010 has 16 bi-directional data lines for the communication of information to and from the processor. Provision is made for 8 16-bit input ports and 8 16-bit output ports for communication to peripheral devices. The port address appears on the 3 least significant address lines.

Communication between the microprocessor and peripherals are controlled by two lines which are active low,  $\overline{DEN}$  (data enable) and  $\overline{WE}$  (write enable).  $\overline{WE}$  is unfortunately not only used for writing data to an output port, it is also used when writing to memory. A new, unambiguous communication line,  $\overline{OUT}$  will be defined. Although this is not a line provided by the TMS32010, its generation will be explained in Section 7.3.2.

The TMS32010 has two lines available for interrupt driven systems,  $\overline{\text{INT}}$  (interrupt) and  $\overline{\text{BIO}}$  (I/O branch control). In the prototype speed measuring instrument it was found that only one 'interrupt' was necessary, and the  $\overline{\text{BIO}}$  line was chosen for this purpose.

In summary, then, the TMS32010 lines that will be used in the interfacing are:

D0-D15	16 Data Lines
PA0-PA2	3 Port Address Lines
$\overline{\text{DEN}}$	Data enable (Input enable)
$\overline{\text{OUT}}$	Output enable
$\overline{\text{BIO}}$	Interrupt

It is important that the timing requirements of the TMS32010 communication lines are adhered to. Although the TMS32010 clock cycle is 200ns the processor utilises a modified Harvard architecture with a 'pre-fetch' and 'fetch' occurring during a single clock cycle. This means that only 100ns is available for data access. In order to give a safety margin the TMS32010 manufacturers recommend that data access times be kept below 70ns.

A copy of part of the data sheet for the TMS32010 is included in Appendix D. A more detailed explanation of the TMS32010 communication lines and timing requirements can be found in the TMS32010 User's Guide [19].

#### 6.1.3 MODULAR DESIGN

It was expected that a number of changes would be made to the interfacing circuitry before an optimum solution would be found. For this reason a modular design approach was adopted. This was implemented in Hardware by the use of a Eurocard Frame System. The use of a Eurocard Frame allowed

each part of the circuitry to be built on its own card and tested before being plugged into the complete system. Communication between the cards was made via a backplane which also held the mating sockets for each card's 64-way connector. Five cards were constructed for the system. Their functions are shown in Figure 6.2.

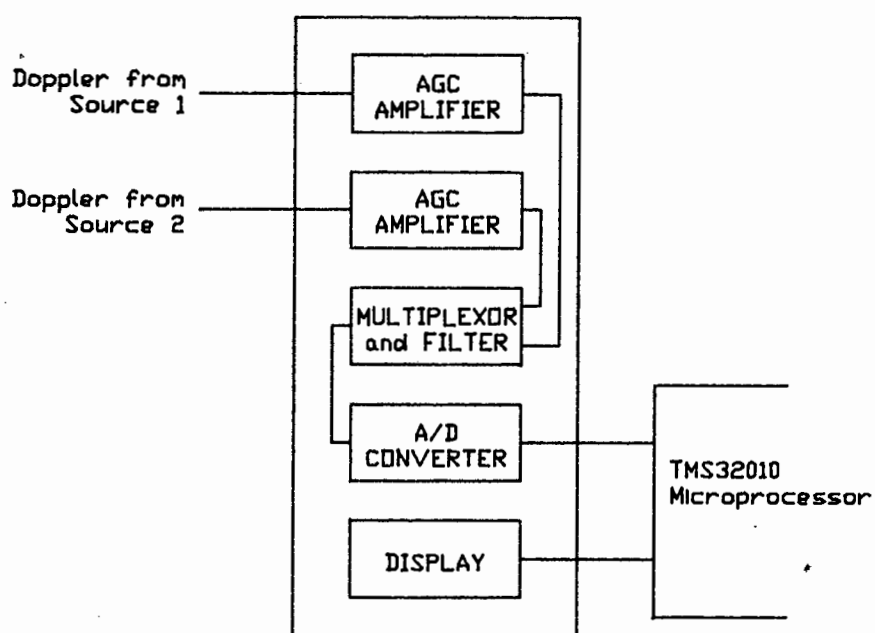


FIGURE 6.2 EUROCARD FRAME SYSTEM CARDS FOR SPEED MEASURING INSTRUMENT

### 6.2 DOPPLER PRE-AMPLIFIER

It was shown in Section 5.6.2 that the noise of the IF amplifier is a major contributing factor to the noise figure of the system.

The low-noise amplifier that follows the mixer is built around an ultra low-noise amplifier, the OP-37. The OP-37 is inexpensive and features incredible noise performance,  $3\text{nV}/\sqrt{\text{Hz}}$  @  $10\text{kHz}$ . It also has an extremely low offset voltage and high gain.

The circuit diagram of the 2-stage doppler amplifier is shown in Figure 6.3.

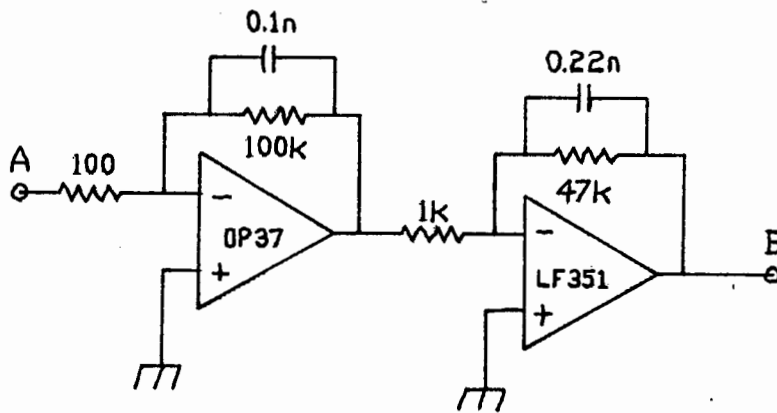


FIGURE 6.3 LOW-NOISE DOPPLER PRE-AMPLIFIER

According to Friis [30] the total noise figure of a multi-stage amplifier is:

$$NF_T = NF_1 + \frac{NF_2}{G_1} + \frac{NF_3}{G_1 G_2} \dots$$

where  $NF_T$  = Total Noise Figure of system

$NF_i$  = Noise Figure of stage  $i$

$G_i$  = Gain of stage  $i$

Thus it can be seen that very little is gained by ensuring low noise in the second amplifier stage as well as the first. The second stage of amplification uses a general purpose LF351 op-amp. Both op-amps are used in the standard inverting amplifier configuration. As the amplifier is

physically close to the mixer a differential amplifier was considered unnecessary.

The input impedance of the low noise amplifier is  $100\Omega$  which is close to impedance of the mixer. The gain of the first stage is 1000 and of the second 47, giving the amplifier a total voltage gain of 93dB. For an input doppler signal with a peak swing of 100uV the output has a peak swing of 4.7V, which with +/- 5V supplies does not quite saturate the second amplifier stage. The low frequency breakpoint of the amplifier is set by R1 and C1 at 200Hz while the opamp feedback capacitors set the upper breakpoint frequency to 15kHz.

In doppler speed measuring instruments rapid amplitude fluctuations of the doppler signals are common. It is possible that these fluctuations could occur too rapidly for the op-amps, resulting in slew-rate limiting. The effects of op-amp slew-rate limiting, together with the effects of clipping, are discussed in Section 8.3.3.

### 6.3 CABLES

A number of techniques were considered for transferring the doppler signals from the microwave sources to the processing unit. Transmission by cable was ultimately chosen as the most reliable technique.

In order to test the system for a number of different values of length L between the sources (see Figure 3.6), it was necessary to make the cables fairly long. A length of 100m was chosen for each cable.

A road is electrically a very noisy environment. Vehicles produce noise over a wide frequency range, from AF to RF. Effective screening of the doppler signals was thus essential. Screened twin-core cable was used with grounding as shown in Figure 6.4. A differential amplifier was used at the receiving end of the cable.

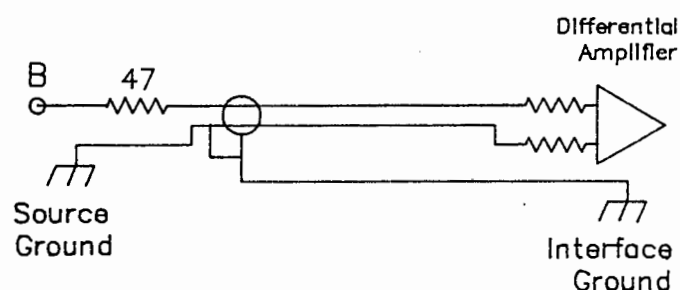


FIGURE 6.4 CABLE GROUNDING TECHNIQUE

The cable has a high series inductance and shunt capacitance and thus it was necessary to include some series resistance in the output of the LF351 to prevent op-amp instability. A  $47\Omega$  resistor in series with the output of the LF351 ensures that the load seen by the op-amp is at least partially resistive.

## 6.4 AUTOMATIC GAIN CONTROL

### 6.4.1 AGC AMPLIFIER REQUIREMENTS

An Automatic Gain Control (AGC) circuit is necessary in order to ensure that the speed measuring instrument can operate with the wide dynamic range of the doppler signals that are presented to it. If there were no AGC in the system, the instrument's dynamic range would be limited to the dynamic range of the A/D converter.

The dynamic range of the AGC was chosen to be 60dB. The AGC time constant must still be determined.

In Microwave Doppler instruments rapid fluctuations of the amplitude of the doppler signals are common [see Section 8.3.4]. These fluctuations are so rapid that they fall within the bandwidth of the doppler signals. It is thus not possible to 'follow' these fluctuations with the AGC without also eliminating the wanted doppler signals.

An obvious choice for the time constant of the AGC is one that just allows the lowest doppler signals to pass. In theory this gives the smallest possible time constant as  $1/f_{\min}$ , where  $f_{\min}$  is the lowest desired doppler frequency. This would, of course, require an infinite order filter so that in practice it is necessary to make the time constant considerably larger than  $f_{\min}$ . In the proposed instrument  $f_{\min} = 300\text{Hz}$  which gives the AGC time constant as  $\gg 3\text{ms}$ .

#### 6.4.2 AGC CIRCUIT

A number of different AGC circuits were considered for use in the speed measuring instrument. The required dynamic range of the AGC, 60dB, is a figure not easily attained with common transconductance amplifiers. For this reason the AGC chosen was based on the principle of electronic attenuation.

The circuit diagram of the AGC circuit is shown in Figure 6.5. Two AGC cards were constructed for the prototype instrument.

The 'heart' of the circuit is a 10-bit, 4-quadrant multiplying Digital-to-Analog converter (DAC), the National DAC1020. The '4-quadrant' capability of this DAC indicates that it is possible to multiply the 10-bit digital word

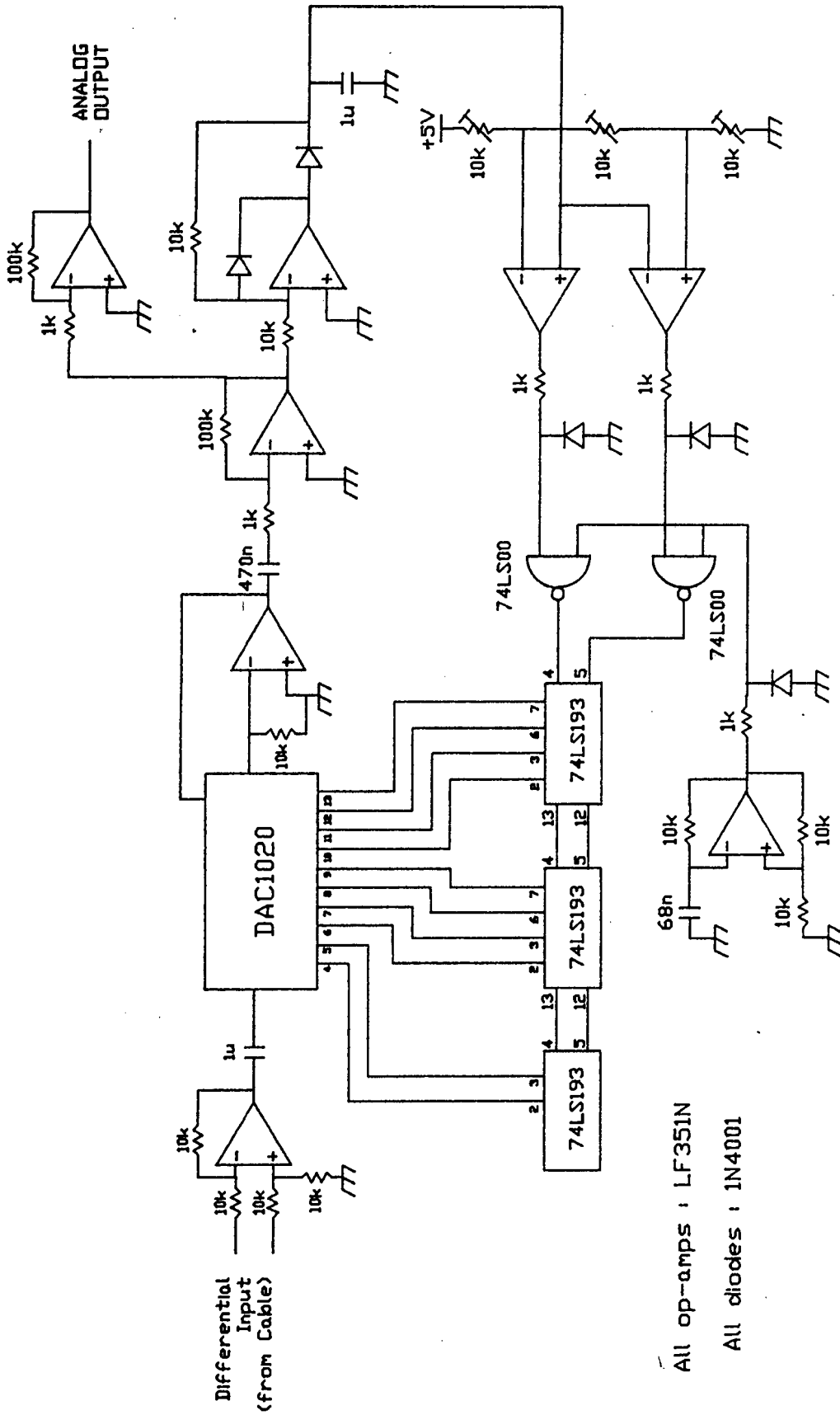


FIGURE 6.5 AGC AMPLIFIER CARD CIRCUIT DIAGRAM  
 (TWO CARDS REQUIRED)

(applied to pins 4 to 13) with a reference signal that is bipolar. It is possible to create electronic attenuators with 2-quadrant multiplying DAC's, but this is more complicated and generally requires that two DACs be used [31].

Included in the circuit diagram of Figure 6.5 is the differential amplifier at the receiving end of the cable carrying the analog doppler signals. After being buffered and amplified, the signal is fed directly into the  $V_{ref}$  input of the multiplying DAC. The amount of attenuation applied to the signal is controlled by a 10-bit digital word. The attenuated signal is then amplified and fed to a precision rectifier, the output of which is low-pass filtered. This filter is partially responsible for the time constant of the complete AGC. The rectified and filtered signal is then fed to a window comparator. This comparator has two digital outputs, both of which are active high. If either output is active it indicates that the signal amplitude is not within the preset window. One of these outputs indicates that the amplitude is too high, and the other that it is low. The digital signals control a three-stage, 10-bit up/down counter comprised of three cascaded 74LS193 counters. The 10 counter lines are connected to the 10 digital control lines of the multiplying DAC, so completing the loop.

The up/down counter is controlled by gating a clock to the 'count up' and 'count down' inputs of the cascaded counters. The frequency of this clock is the second factor which influences the time constant of the AGC loop, as it limits the maximum speed at which the AGC can 'track' amplitude changes. Because of the presence of both the detector filter and the counter, an exact characterisation of this AGC loop is not trivial. The optimum clock frequency was found by experimentation to be approximately 3kHz.

The signal that is extracted from the AGC loop requires further amplification before it is passed to the rest of the interfacing circuitry. One disadvantage of this type of AGC loop is the large amount of amplification required following the electronic attenuator.

In the original design of the AGC loop a further gate was included which allowed the counter to be switched off, thus preventing the loop from 'tracking' while the time data was being read. Amplitude changes in the loop occur very rapidly, however, and the high frequency components that are generated during amplitude 'switching' are filtered out by the anti-aliasing filter [Section 6.6]. It was therefore found unnecessary to 'turn off' the AGC while data was being read.

## 6.5 MULTIPLEXOR

The multiplexor was included in the instrument to prevent unnecessary duplication of parts of the interfacing circuitry. The circuit diagram of the multiplexor is shown in Figure 6.6. This circuitry was included on the anti-aliasing filter card.

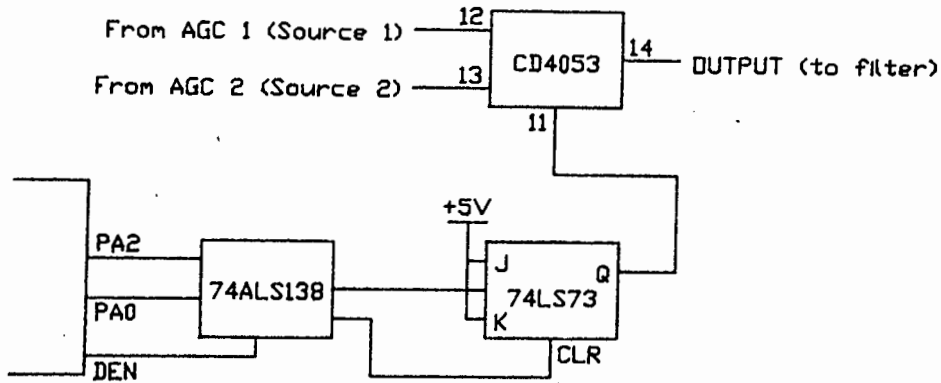


FIGURE 6.6 MULTIPLEXOR CIRCUITRY (INCLUDED ON FILTER CARD)

The output lines of the 74ALS138 decoder set and reset a 74LS73 flip-flop which toggles a CD4053 2-into-1 multiplexor. The 74ALS138 is wired so as to give Source 1 the 'input address' 01 and Source 2 the 'input address' 02.

## 6.6 ANTI-ALIASING FILTER

### 6.6.1 INTRODUCTION

According to Shannon, sampling of a signal must occur at a rate greater than twice the highest frequency in the signal. This constraint on the sampling frequency can be expressed as :

$$f_s > 2 f_{max}$$

where:  $f_s$  : Sampling frequency

$f_{max}$  : Highest frequency in the signal being sampled.

If this criterion is not met, 'aliasing' occurs. Aliasing is ambiguity regarding the true frequencies of signals of

higher frequencies than  $f_{\max}$ . In the discrete transformed waveform, aliasing manifests itself as frequency components smaller than  $f_{\max}$  that were not present in the original analog signal. It is thus important in sampled data systems to ensure that aliasing does not occur, and for this purpose anti-aliasing filters are used.

#### 6.6.2 ANTI-ALIASING FILTER REQUIREMENTS

Before an anti-aliasing filter for the speed measuring instrument can be designed, it is necessary to know the sampling frequency of the system, maximum frequency (speed) that will be measured and the dynamic range of the A/D converter. The choice of these parameters is discussed in Sections 7.4.2.2. ( $f_s$  and  $f_{\max}$ ) and 4.5.2 (dynamic range) and here are merely stated in order to determine the filter requirements:

Sampling frequency : 22 755 kHz

Maximum frequency to be measured : 8 893 kHz (200 km/h)

A/D converter dynamic range : 50 dB

The anti-aliasing filter must ensure that no frequency greater than 11378 kHz ( $1/2 f_s$ ) with amplitude greater than -50dB (referenced to maximum possible signal amplitude) can arrive at the A/D converter. The maximum allowable passband ripple was chosen to be 0.1dB. The filter requirements are shown in Figure 6.7.

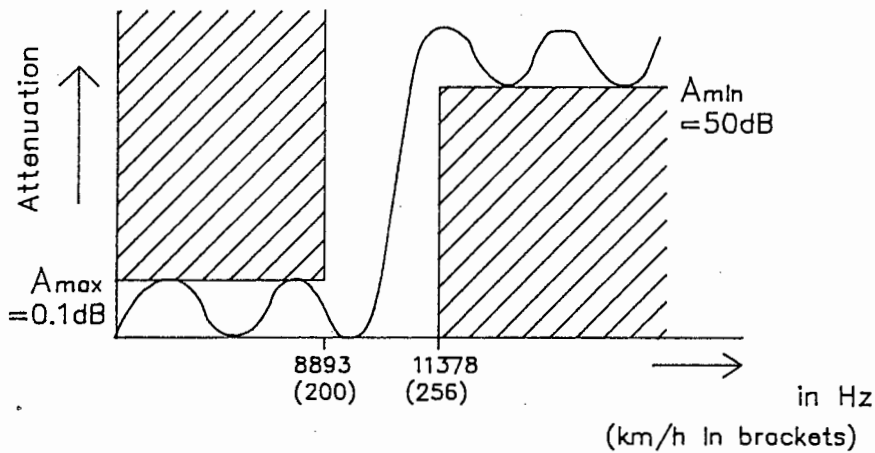


FIGURE 6.7 ANTI-ALIASING FILTER REQUIREMENTS

### 6.6.3 FDNR FILTERS

Passive filters have the disadvantage that inductors must be wound and in general 'tuned'. At low frequencies (up to AF) inductors become large and lossy and thus have low  $Q$  which makes the realisation of high order filters at low frequencies a difficult task.

In 1968 Bruton [32] proposed what is now known as the Bruton Transformation for the elimination of inductors from filters. The Bruton Transformation is the  $1/s$  transformation whereby resistors become capacitors, inductors become resistors and capacitors become frequency dependant negative resistors (FDNR's). Certain realisations of the FDNR (such as the one presented below) exhibit very high  $Q$ , much higher than the equivalent passive inductor.

A popular (and high  $Q$ ) realisation of the FDNR is shown in Figure 6.8. In this realisation, one side of the FDNR must be grounded. Circuits for 'floating' FDNR's exist, but they are in general more complex [33,34].

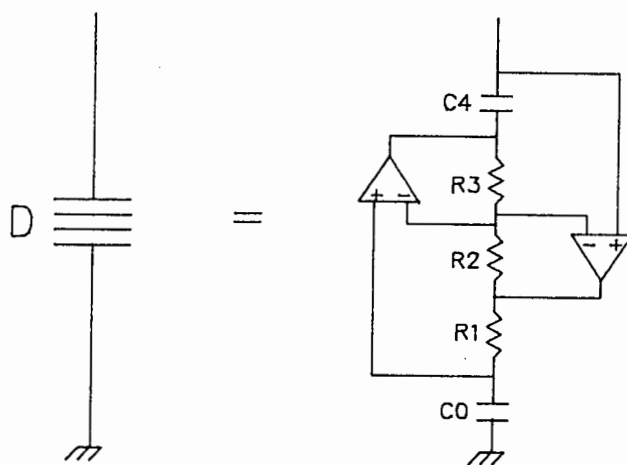


FIGURE 6.8 REALISATION OF GROUNDED FDNR

In this realisation of the FDNR,

$$D = \frac{C_0 C_4 R_3 R_1}{R_2}$$

#### 6.6.4 FILTER REALISATION

A 7th order elliptic filter, with  $\rho=15\%$ , and  $\theta=55^\circ$ , selected from standard filter design tables, meets the requirement. The theoretical stopband attenuation of this filter is better than 53dB at frequencies higher than 11383 Hz.

Figure 6.9 shows the minimum capacitor passive realisation of this filter (which gives the minimum number of FDNR's after the Bruton transformation).

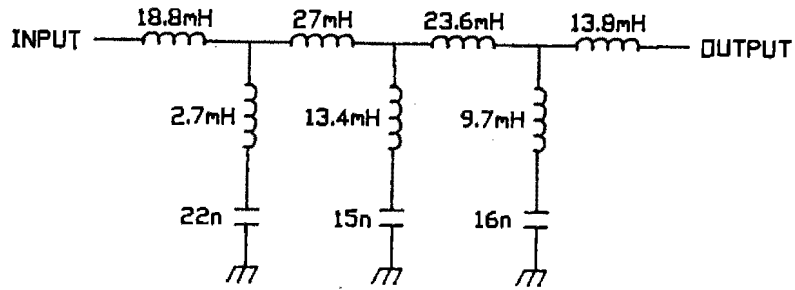


FIGURE 6.9 PASSIVE REALISATION OF ANTI-ALIASING FILTER

The input and output of the filter were matched to an impedance of  $1k\Omega$ .

The complete circuit diagram of the FDNR realisation of this filter is shown in Figure 6.10, and the response of the filter in Figure 6.11.

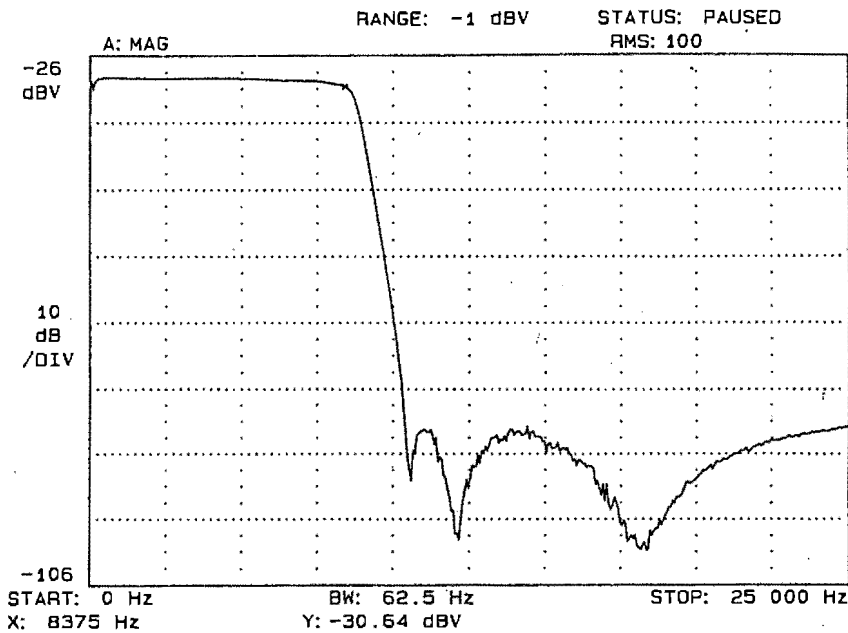
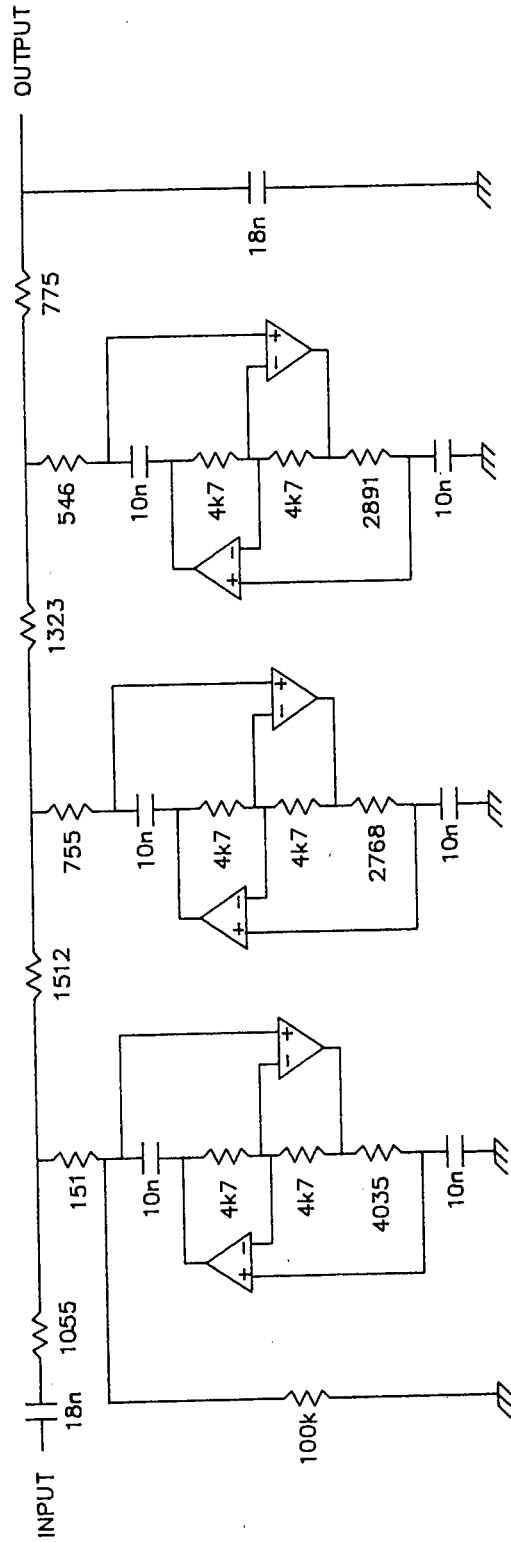


FIGURE 6.11 ANTI-ALIASING FILTER RESPONSE

It can be seen that the filter meets the requirements of Figure 6.7. The  $100k$  resistor is necessary in order to bias the signal. This effectively adds a pole at the origin,



**FIGURE 6.10 ANTI-ALIASING FILTER CARD CIRCUIT DIAGRAM**

which, in the speed measuring instrument, is of no consequence. Other (and more complex) biasing arrangements are possible if the pole at the origin is undesirable.

## 6.7 ANALOG TO DIGITAL CONVERTER

The Analog-to-digital converter chosen for use in the instrument is the (relatively) inexpensive 8-bit National ADC0820. This is a 'flash' converter, featuring a very fast conversion time of 500ns, and thus allowing sampling rates of up to 2MHz. The circuit diagram of the A/D converter is shown in Figure 6.12.

Although the ADC0820 has a latched tri-state output, the access time (from tri-state to data valid) is too long to interface it directly to the TMS32010. For this reason a secondary buffer, a 74ALS244 was used.

The A/D is used in 'stand-alone' mode. The conversion rate is determined by the 555 oscillator. The 74LS221 monostable turns the oscillator square wave into a train of low 10us pulses, thus satisfying the timing requirements of the WE pin. During conversion the INT pin on the ADC0820 goes high. 50ns (max) after INT goes low the data is available and thus this line is fast enough to signal "data ready" to the TMS32010. To prevent reading of the same data twice a flip-flop is necessary which is set by INT (ADC0820) and cleared when the data is read by the TMS32010. The Q output of the flip-flop is connected to the TMS32010 BIO line to indicate 'data ready'.

In a commercial speed measuring instrument the 555 RC oscillator that determines the conversion rate would be unacceptable, as the poor long-term frequency stability of

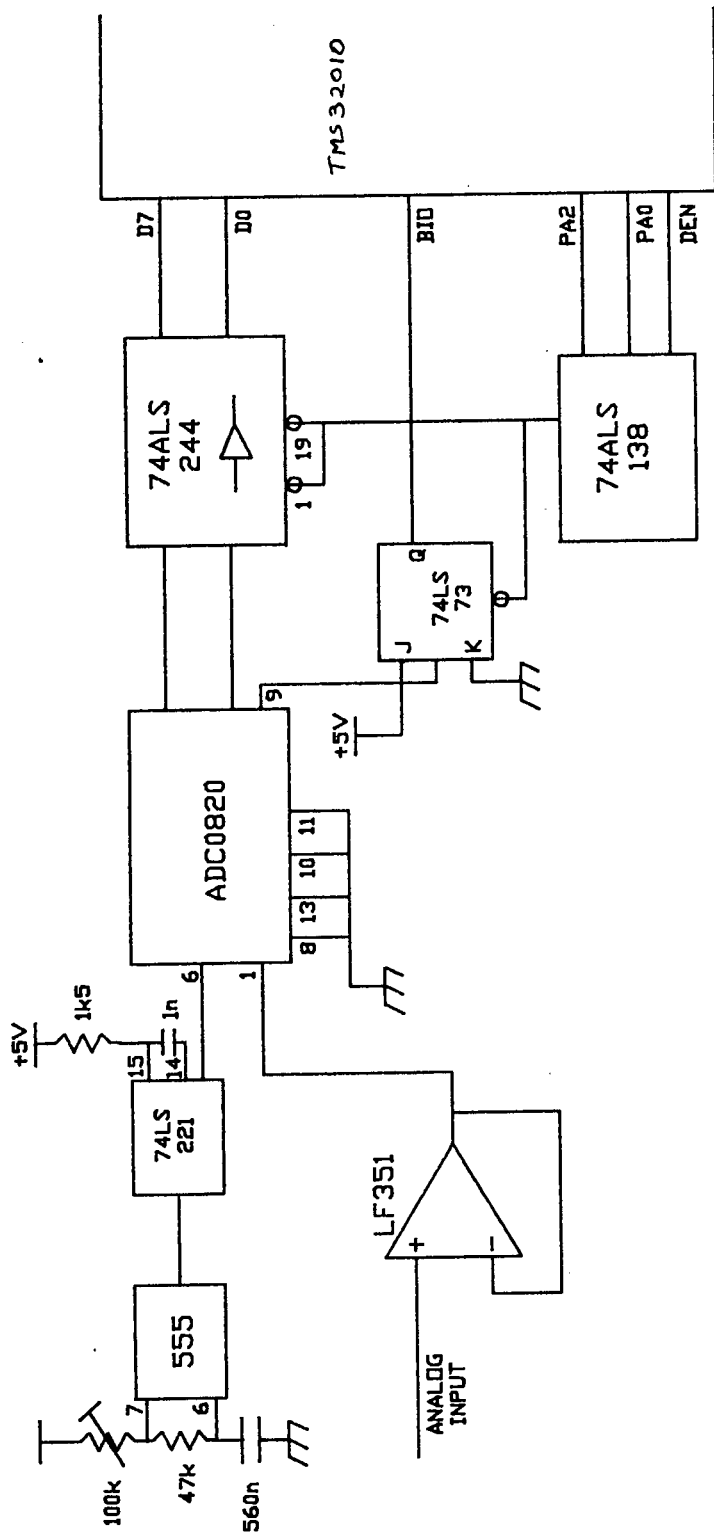


FIGURE 6.12 A/D CONVERTER CARD CIRCUIT DIAGRAM

this oscillator would degrade the accuracy of the instrument. It suffices, however, for the prototype instrument.

## 6.8 DISPLAY CARD

The circuit diagram of the display card is shown in Figure 6.13. The maximum 'displayable' speed is 199km/h.

7-Segment LED displays, MAN74's, were used on the display card. The 9 data lines from the TMS32010 (D0-D8) are latched using 74LS75's. Two 74LS47 decoder-drivers control the lower two display digits. The most significant digit is hardwired to read '1', and is either on or off. Latching is controlled by a 74ALS138 which is wired to give the display card the output address '02'.

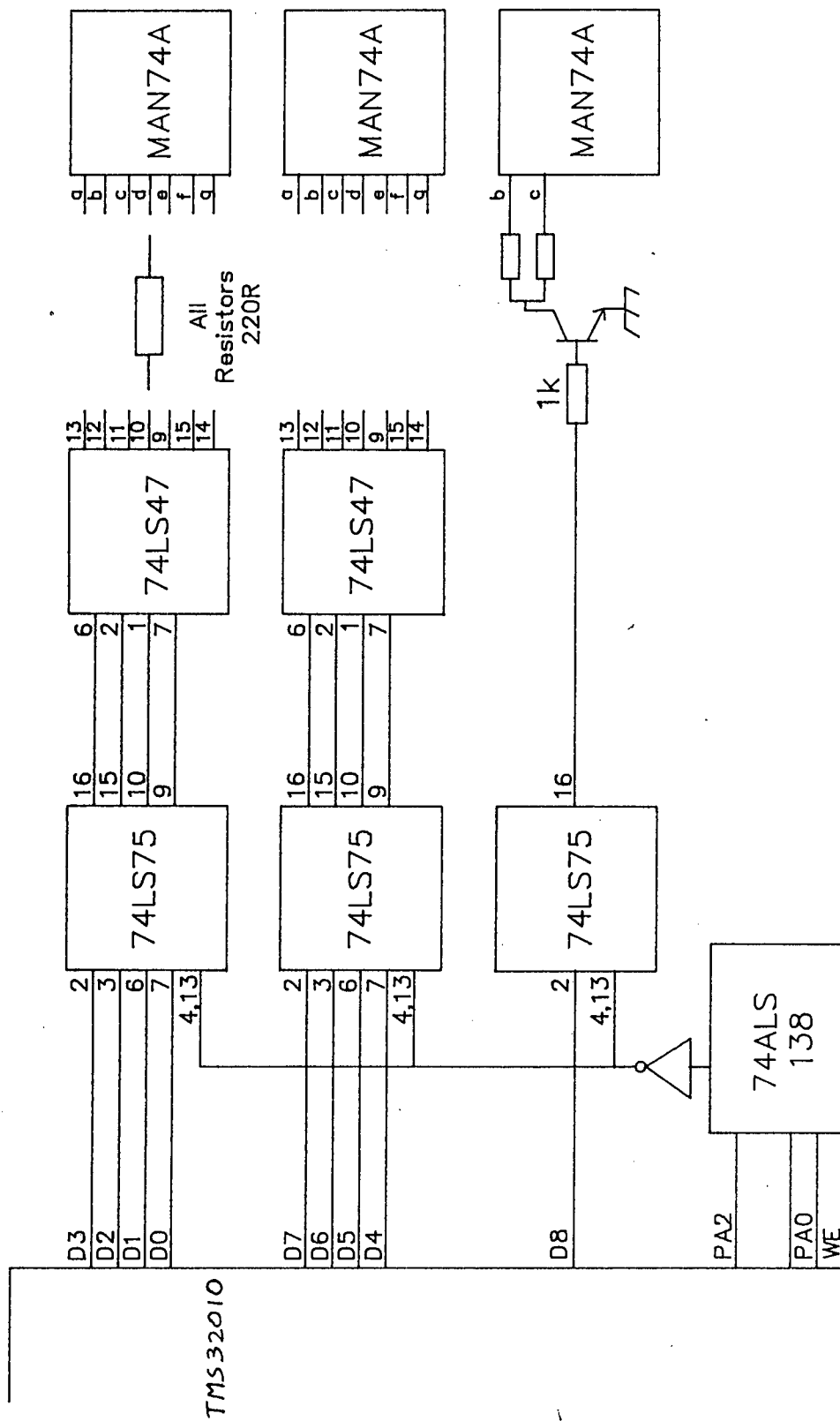


FIGURE 6.13 DISPLAY CARD CIRCUIT DIAGRAM

## CHAPTER 7 : SIGNAL PROCESSING

### 7.1 THE FOURIER TRANSFORM

#### 7.1.1 INTRODUCTION

The Fourier Transform (FT) and its inverse, the Inverse Fourier Transform (IFT), have long served as the 'bridges' between the time domain and the frequency domain and are discussed at some length in the literature [35,36].

The Fourier Transform Pair (FT and IFT) can be written in the form :

$$X(f) = \int_{-\infty}^{\infty} x(t) e^{-i2\pi ft} dt$$

$$x(t) = \int_{-\infty}^{\infty} X(f) e^{i2\pi ft} df$$

for  $-\infty < f < \infty$ ,  $-\infty < t < \infty$  and  $i = \sqrt{-1}$

where  $x(t)$  : Time domain continuous signal

$X(f)$  : Frequency domain continuous signal

#### 7.1.2 THE DISCRETE FOURIER TRANSFORM

The FT and IFT can operate only on continuous waveforms and as such are of limited value in the transformations of real signals. For this reason the discrete counterparts of the FT and IFT, the Discrete Fourier Transform (DFT) and Inverse Discrete Fourier Transform (IDFT), were developed. The discrete Fourier pair that applies to sampled versions of

the continuous waveforms described above can be written in the form:

$$X(j) = \frac{1}{N} \sum_{k=0}^{N-1} x(k) e^{-i2\pi jk/N}$$

$$x(k) = \sum_{j=0}^{N-1} X(j) e^{i2\pi jk/N}$$

for  $j = 0, 1, 2, \dots, N-1$

$k = 0, 1, 2, \dots, N-1$

and  $x(k)$ ,  $X(j)$  complex series.

The derivation of these equations is not given in this dissertation but are amply covered in the literature. It is convenient when evaluating the DFT to replace  $e^{2\pi i/N}$  with  $W_N$ , which gives the DFT pair as :

$$X(j) = \frac{1}{N} \sum_{k=0}^{N-1} x(k) W_N^{-jk}$$

$$x(k) = \sum_{j=0}^{N-1} X(j) W_N^{jk}$$

It must be remembered that the DFT of a sampled data series is simply an estimate of the FT of the corresponding continuous waveform. How good an estimate it is depends on the number of points,  $N$ , in the series.

When evaluating the DFT the sampled time series  $x(k\delta T)$ , where  $\delta T = 1/f_s$  ( $f_s$  = sampling frequency), is assumed to be periodic in the time domain with a period  $T$ ,  $T = N\delta T$ . The time series  $x(k)$  is complex and the DFT of this series results in the complex series  $X(jf_0)$ , where  $f_s = Nf_0$ .

Although the DFT allows computation of the FT by computer it has one serious drawback: the number of arithmetic operations required for evaluation of the DFT is high. In the DFT the number of arithmetic operations required to evaluate an N-point transform is proportional to  $N^2$ . For many years calculation of the DFT was limited to mainframe computers, particularly when N was large.

### 7.1.3 THE FAST FOURIER TRANSFORM

In 1965 Cooley and Tukey published an algorithm for the efficient calculation of the Discrete Fourier Transform [42]. This algorithm, now known as the Fast Fourier Transform (FFT), revolutionised the field of Digital Signal Processing. The FFT reduced the number of arithmetical operations required by  $N^2$  :  $N \log(N)$ . Thus, for instance the reduction in operations for a 1024 point transform is 1048576:10240 or approximately 100:1 !

The FFT is discussed in detail in Section 7.4.2.

### 7.1.4 THE DFT AND FFT FOR REAL DATA

When the series  $x(k)$  is real, then the real part of the Fourier Transform of  $x(k)$ ,  $X(f)$ , is symmetric around the folding frequency  $f_f$ , where  $f_f = f_s/2$ . The imaginary part of  $X(f)$  is anti-symmetric about  $f_f$ . Thus the series  $X(j=0,1,\dots,N/2)$  is the complex conjugate of the series  $X(j=N/2,N/2+1,\dots,N)$  and half the information contained in the complete DFT is redundant. These relationships can be expressed as :

$$X(N-n) = X^*(n)$$

and it follows that:  $|X(N-n)| = |X(n)|$

where N : Number of data points  
n : data number

Algorithms exist which improve the efficiency of the FFT by taking advantage of this redundancy [37,38].

## 7.2 POWER SPECTRAL ESTIMATION

### 7.2.1 INTRODUCTION

In Electrical Engineering the greatest application of the Fourier Transform is in the estimation of the Power Spectra of signals, otherwise known as Spectral Analysis. In the proposed Speed-measuring instrument the Signal Processing requirement is fundamentally one of Spectrum Analysis.

Many authors warn against the 'blind' application of the Fourier Transform for the purposes of Spectral Analysis. Bergland [39] identified three main problems encountered in the use of the DFT : aliasing, leakage and the picket-fence effect. Aliasing was discussed in Section 6.3 and will be prevented by the use of the Anti-aliasing filter described in that Section. Leakage and the 'picket-fence' effect are more serious problems and will be discussed in some detail. The following explanations of these problems are summaries of the descriptions presented by Bergland.

### 7.2.2 LEAKAGE AND WINDOWING

The problem of leakage arises because the sampled time series is a finite record of length T seconds. All signals that occurred outside of this time period are ignored. This

is equivalent to multiplying the infinite length continuous time waveform by a rectangular window of length T as shown in Figure 7.1.

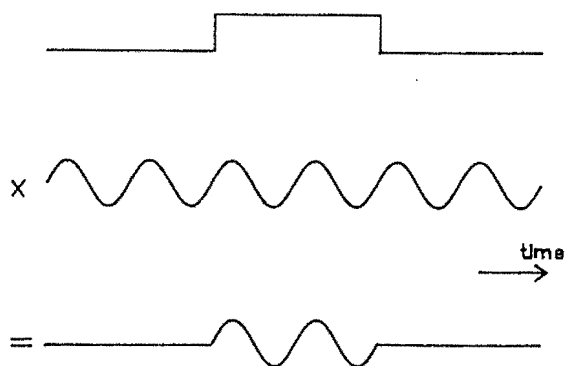


FIGURE 7.1 THE RECTANGULAR WINDOW FOR RECORD AQUISITION

The relationship between the continuous waveform and the finite record can be expressed as :

$$r(t) = s(t)w_r(t)$$

where  $r(t)$  : the data record of length T  
 $s(t)$  : the continuous time waveform  
and  $w_r(t)$  : the rectangular data window

Multiplication in the time domain is equivalent to convolution in the frequency domain. Thus the net result of this 'windowing' is to convolve each spectral line in the frequency domain with the Fourier Transform of the rectangular window, a  $(\sin x)/x$  function.

The time record can now be expressed as:

$$R(f) = S(f) * W_r(f)$$

where  $R(f)$  : Fourier Transform of time record

$S(f)$  : Fourier Transform of continuous time signal

$W_r(t)$  : Fourier Transform of Rectangular Window

Leakage arises from:

(i) The finite width of the main lobe, and

(ii) The presence of sidelobes. In the case of the rectangular window the first sidelobe is only 13dB down from the main lobe.

In the prototype speed measuring instrument the effect of the finite width of the main lobe would be to reduce the ability of the system to discriminate between different vehicles. The presence of sidelobes, however, could have more serious consequences as they would appear to the instrument as different vehicles.

One method of alleviating the problem of leakage is to multiply the continuous time waveform by a window that is not rectangular. The advantage of this is that a window can be selected whose Fourier Transform has a narrow main lobe and low sidelobe levels. A large number of windows have been proposed for this purpose [40,41]. The window used in the prototype speed measuring instrument is discussed in Section 7.4.4.

### 7.2.3 THE 'PICKET-FENCE' EFFECT

The 'picket-fence' effect is best explained by modelling the Discrete Fourier Transform as a set of  $N$  independent

filters, the Q of each being dependant on the data window that was applied. If the frequency being transformed lies at the centre frequency of one of these filters, the amplitude of the signal is accurately represented. If, in the worst case, the signal is at a frequency halfway between two filters, the amplitude of the signal will appear much smaller than its true value. In the case of a rectangular window this amplitude may be as low as 60% of the true amplitude (voltage), or in the case of the power spectrum, appear to have only 40% of the power.

One solution to this problem is to 'pad out' part of the original time record which are equal to zero. No discussion of this technique will be given here, but it can be shown [40] that padding with zeroes enables the calculation of the Fourier components between the original harmonics. A disadvantage of this is that it increases the size of the Fourier Transform that must be computed. This means an increase in both computational time as well as memory.

Bergland points out that in many cases this problem may not be as serious as it appears; it must, however, be borne in mind in Discrete Fourier Analysis.

It has been shown [Section 2.4.2] that in the proposed speed measuring instrument very little information is contained in the amplitude of the signal. For this reason no compensation for the 'picket-fence' effect was included in the instrument.

## 7.3 SIGNAL PROCESSING HARDWARE

### 7.3.1 EVALUATION MODULE

The manufacturers of the TMS32010, Texas Instruments, offer an evaluation board for the TMS32010. This board, the TMS32010 EVM (referred to from here on as the EVM), features an on-board monitor program for editing, debugging and evaluating programs for the TMS32010. The EVM has two fully configurable serial ports, which can be used to interface the board to a computer terminal, a printer, an IBM personal computer, or any other external device with RS232 communication.

The EVM also has the facility for storing assembled TMS32010 programs on EPROM, thus retaining the programs when the power to the board is switched off. A TMS32010 'emulation' cable is provided, which simulates all 40 pins of the TMS32010 IC.

Although the EVM is physically large, it was used as the Hardware Signal Processor for the prototype Speed measuring instrument. It was ideal for this application as a battery operated terminal could be operated with the EVM and so allow 'on-site' optimisation of the Signal Processing Software.

The power supply requirements of the EVM are 5V @ 2A, +12V @ 100mA and -12V @ 100mA, which were easy to generate with batteries. The emulation cable, a 40-way ribbon cable, was used to connect the EVM to the Eurocard frame containing the interfacing circuitry.

### 7.3.2 OUT GENERATION

Unlike the TBLR and IN commands, the TBLW and OUT commands of the TMS32010 use the same control lines. Thus OUT 0,3 performs exactly the same function as TBLW 0,3. To avoid this problem a new control line,  $\overline{\text{OUT}}$ , was generated.  $\overline{\text{OUT}}$  is low when  $\overline{\text{WE}}$  is low and the Address lines A3 to A11 (all non port address lines) are low. The OUT circuitry is shown in Figure 7.2.

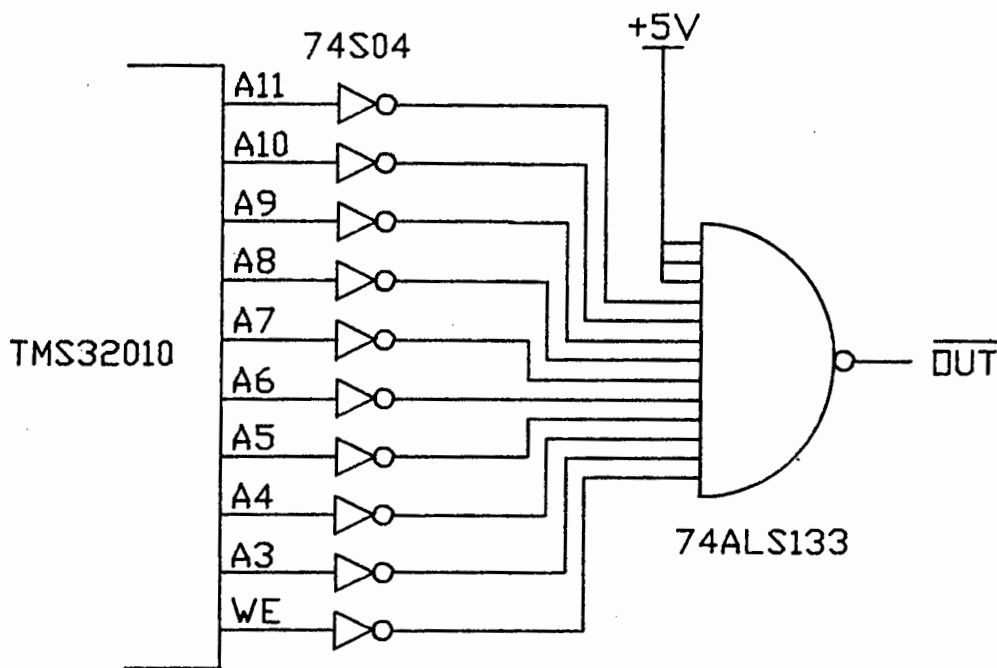


FIGURE 7.2 GENERATION OF OUT CIRCUITRY

The  $\overline{\text{OUT}}$  circuitry was included in the box containing the interfacing circuitry.

## 7.4 INTRODUCTION TO THE SIGNAL PROCESSING REQUIREMENTS OF THE SPEED MEASURING INSTRUMENT

### 7.4.1 SIGNAL PROCESSING BLOCK DIAGRAM

The block diagram of the speed-measuring instrument signal processing is shown in Figure 7.3.

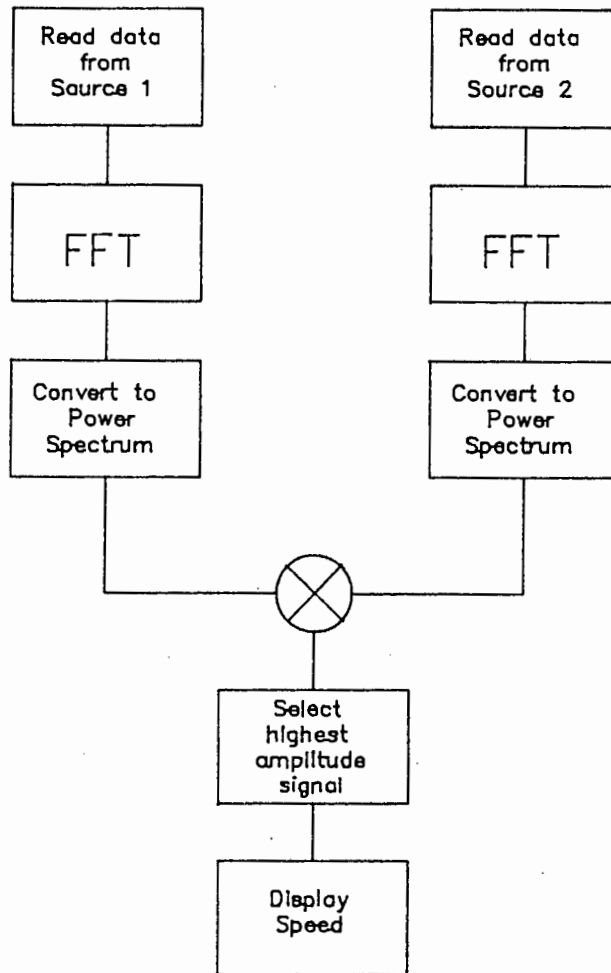


FIGURE 7.3 SIGNAL PROCESSING REQUIRED FOR THE SPEED MEASURING INSTRUMENT

The signal processing is based on the Fast Fourier Transform algorithm. This aspect of the processing is discussed first.

#### 7.4.2 THE FFT ALGORITHM

##### 7.4.2.1 THE COOLEY-TUKEY ALGORITHM

The original FFT algorithm proposed by Cooley and Tukey operates on  $N$  complex points, where  $N$  is a power of two. The algorithm is arranged in such a way that the Fourier transformed series occupies the same storage locations as the original time series. Thus only  $2N$  storage locations are required ( $N$  real and  $N$  complex), although, of course, the original series is destroyed.

Since the Cooley-Tukey FFT algorithm was published [42], many other FFT algorithms have been proposed [43,44,45]. These algorithms differ from the original one in terms of :

- a) The number of points they can operate on,
- b) The number of arithmetic operations required for a transform of length  $N$ ,
- c) The number of storage locations required.

The Cooley-Tukey algorithm still remains one of the easiest of the FFT algorithms to implement in software and is the one used in the prototype speed measuring instrument, although for the same number of points more efficient algorithms do exist.

The Cooley-Tukey algorithm for  $N=8$  is shown diagrammatically in Figure 7.4.

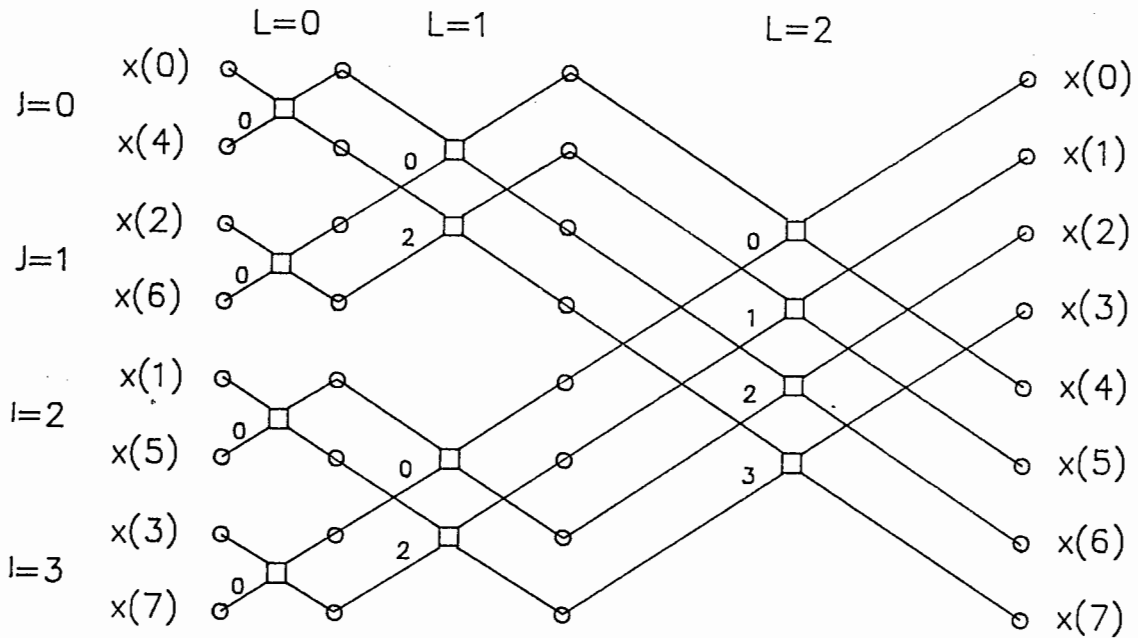


FIGURE 7.4 THE COOLEY-TUKEY 'IN-PLACE, DECIMATION-IN-TIME' FFT ALGORITHM FOR N=8.

Due to the computation order of this particular algorithm, it is known as a 'Radix-2, in-place, Decimation-in-time' Algorithm. As can be seen, the algorithm is made up of a number of 'butterflies', so-called because of their shape. The inputs to a 'butterfly' are  $x(I)$  and  $x(I2)$ , and the outputs are  $x'(I)$  and  $x'(I2)$ , where:

$$\begin{aligned} x'(I) &= x(I) + x(I2)W^t \\ x'(I2) &= x(I) - x(I2)W^t \end{aligned}$$

In these equations  $W^t$  is the 'phase coefficient' as shown in Section 7.1.2. The variable 't' is known as the 'twiddle factor'.

The FFT butterfly is shown in Figure 7.5.

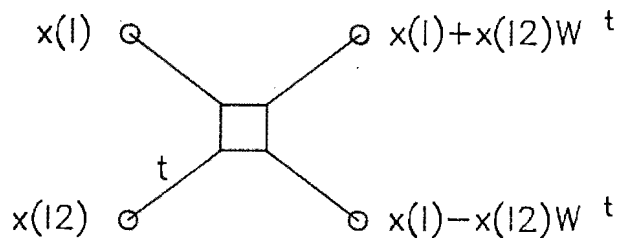


FIGURE 7.5 THE FFT BUTTERFLY

The algorithm requires that the data be input not in sequence, but in 'bit-reversed' order. Thus, for instance, the second data sample that must be input to the algorithm is the actually the fifth, not the second. 'Bit-reversal' is a feature of all FFT algorithms and must occur somewhere in the algorithm. In the speed measurement system it is convenient to apply the 'bit-reversal' at the input to the algorithm, as will be shown in Section 7.5.2.2.

In this dissertation no attempt is made either to derive the Cooley-Tukey FFT algorithm, as this is well covered in the literature. The algorithm is presented in flowchart form in Section 7.4.2.3.

#### 7.4.2.2 THE CHOICE OF N AND F<sub>S</sub>

In the speed measuring instrument the resolution required is 1km/h. In order to measure speeds of up to 200 km/h with this resolution, at least 200 points in the frequency domain are required. It is convenient to allow each frequency point to represent 1km/h. The Cooley-Tukey algorithm requires that N be a power of two, so this gives the number of unambiguous frequency points required as 256.

It has been shown that for real input data (such as doppler signals), half of the points resulting from the Fourier

Transform are redundant. Thus in order to obtain 256 unambiguous frequency points, 512 real time points are required.  $N = 512$  is the value chosen for the prototype instrument.

The doppler frequency resulting from a vehicle travelling at 256 km/h is 11378 kHz. In order to satisfy the sampling theorem, the sampling frequency is given by  $2 \times 11378$ , or  $f_s = 22755$  Hz. This is the sampling frequency used in the system. The maximum frequency that is required to be measured is that corresponding to a speed of 200 km/h, or 8893 Hz. This gives  $\Omega_s$  for the anti-aliasing filter as  $256/200$ , or 1.28.

#### 7.4.2.3 FFT FLOWCHART

The flowchart of one possible implementation of the Cooley-Tukey FFT algorithm is given in Figure 7.6. This is the implementation used in the prototype software.

During the years that FFT algorithms were written solely in FORTRAN, the indices I, I2, J, K, L, M, N (all integers in FORTRAN) used in the algorithm became standard and are still often used.

The array x contains the time data at the start of the program and the frequency data at the end. The time data is lost. Both W and the array x are complex. N is the number of data points, and L2N is the log to the power of 2 of N.

In a complete FFT blocks 8, 9, 10 and 11 in Figure 7.6 are repeated many times, and it is thus important in terms of processing speed that these parts of the program in particular are efficiently coded. The most important of these blocks is block 9, which contains the FFT 'butterfly'.

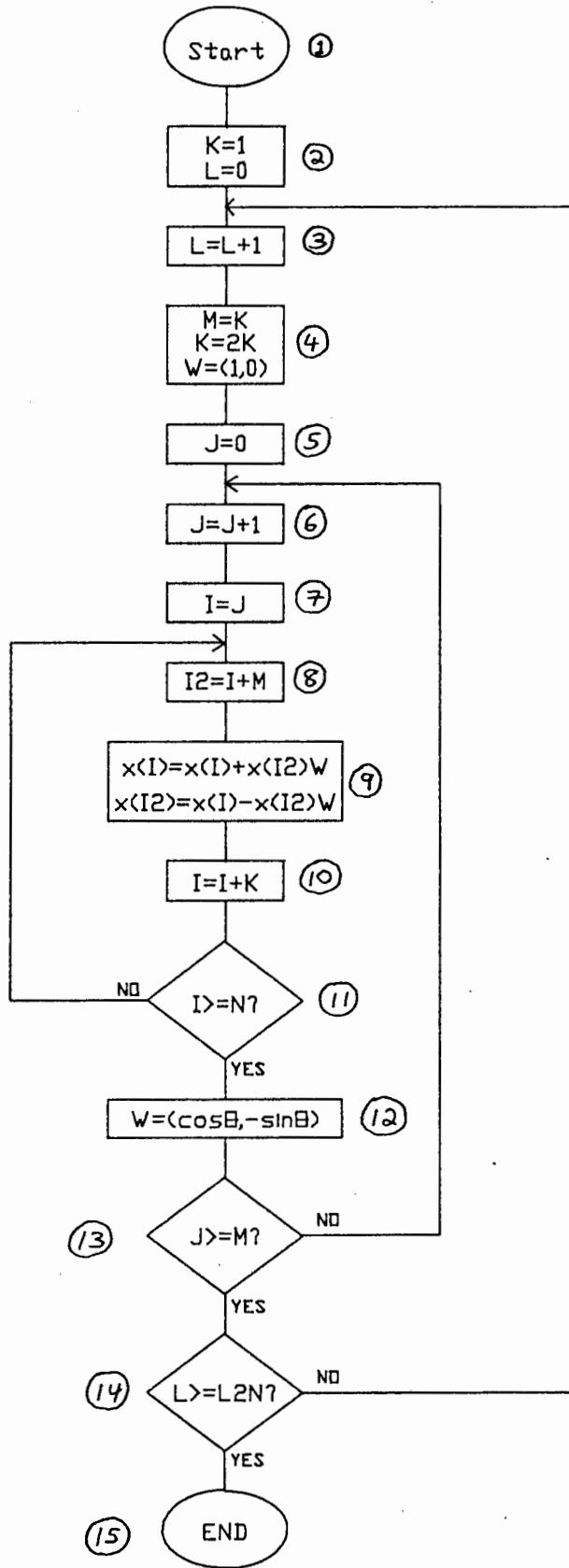


FIGURE 7.6 FFT FLOWCHART

### 7.4.3 DATA ACQUISITION

The first function of the signal processor is to read and store the signals provided by the Microwave Sources. It is important that the data from the sources is read into the processor at approximately the same time. If the data were read at substantially different times, changes in vehicle speeds due to acceleration or deceleration could cause a single vehicle to appear to the processor as two different vehicles.

With the analog circuitry shown in Figure 6.1, time division multiplexing (TDM) of the signals is not possible due to the relatively slow step response of the filter. TDM would only be possible if separate filters were used, and the multiplexor placed after the filters. This would, however, increase the system complexity.

The time to read an entire 'record' of data from one Microwave Source is given by :

$$T_{acq} = \frac{N}{f_s}$$

where  $T_{acq}$  is the time to read a record (acquisition time),  $N$  is the number of data points, and  $f_s$  is the sampling frequency.

For the speed measurement system, where  $N=512$  and the sampling frequency is 22755 kHz, the acquisition time is 22.5ms. In the system signal processor the data from the two sources are read sequentially, or within 22.5 ms of each other. A vehicle travelling at 200km/h has travelled only 1.25m in 22.5ms, and thus this method of reading the data was considered adequate.

#### 7.4.4 WINDOWING

In order to avoid the problems of leakage described in Section 7.2.2, a non-rectangular window was applied to the incoming data. As is shown in Section 7.5.1.2, there is stored in the Program Memory of the signal processor a table of sine and cosine coefficients. It is convenient to use these coefficients in order to apply a window to the data whose Fourier Transform has a narrow main lobe and small sidelobes. The applied window is shown in Figure 7.7.

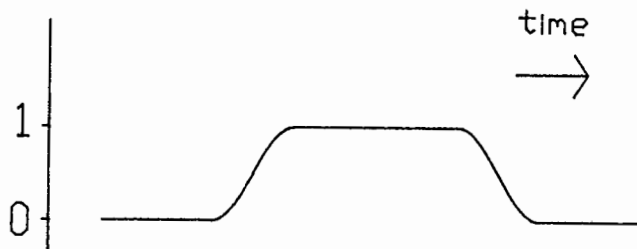


FIGURE 7.7 TIME FUNCTION WINDOW USED IN SIGNAL PROCESSOR

This window is similar to the Blackman Window, well known for its extremely low sidelobe levels (better than -80dB). It can be shown that the window of Figure 7.7 has a sidelobe suppression of better than 50dB, the dynamic range of the A/D converter.

#### 7.4.5 CONVERSION TO POWER SPECTRA

After the FFT, the frequency series must be converted to a Power Spectrum before any further processing can be done. The power in any point  $X(j)$  is given by :

$$P(j) = \sqrt{(X_r(j))^2 + (X_i(j))^2}$$

where  $P(j)$  : The power  
 $X_r(j)$  : The real part of  $X(j)$   
 $X_i(j)$  : The imaginary part of  $X(j)$

In TMS32010 code squaring is a relatively simple operation, but taking the square root of a number is not. For this reason the conversion to the Power Spectrum in the signal processor is performed merely by squaring and adding the real and imaginary parts of each frequency point. Although not strictly indicative of the power contained in each point, this method will suffice as there is very little information contained in the amplitude of the doppler signals.

#### 7.4.6 SELECTING THE DISPLAYED SPEED

After the discrete Power Spectra of the doppler signals from the two Sources have been obtained, the Spectra are multiplied together to give a Spectrum which contains only the vehicle speeds 'seen' by both sources. In the simplest implementation of the proposed speed measurement system the speed (frequency) with the highest amplitude is displayed.

There are primarily two advantages to be gained by further processing:

- (i) The ability of the system to distinguish between vehicles and noise can be controlled.
- (ii) The system can be made to reject readings if there appears to be more than one vehicle in the 'Capture Area'.

In order to achieve the advantages listed above, a system 'Signal-to Noise' ratio can be measured. This measurement is made by calculating the amplitude difference between the

highest amplitude signal and the second highest signal. On the basis of the value obtained for the 'Signal-to-noise' ratio the speed measurement is either accepted or rejected. In this system no distinction is made between unwanted vehicles and noise.

## 7.5 SIGNAL PROCESSING SOFTWARE

### 7.5.1 INTRODUCTION

#### 7.5.1.1 PROGRAM EFFICIENCY

As speed measurements must be made in virtually real time, it is important that the signal processing, from data acquisition to the display of the speed, be as fast as possible.

By far the greatest proportion of time used by the signal processor is the time spent calculating the FFT. In the FFT itself most of the time is spent computing the FFT butterflies, or blocks 8,9,10 and 11 in Figure 7.6. In a 512-point transform these blocks are executed a total of 2304 times. The TMS32010 instruction cycle time is 200ns, and thus each instruction in one of these blocks adds  $2304 \times 200\text{ns}$ , or approximately 0.5ms to the total computation time. It is thus important that the code in these blocks in particular is written as efficiently as possible.

Because the bulk of the processing time is consumed by the FFT, very little effort was expended in making the rest of the software time-efficient. In the rest of the software the emphasis was placed rather on flexibility and ease of programming. Thus, except for the FFT routine, the software is not written efficiently.

### 7.5.1.2 MEMORY ALLOCATION

A 512-point Cooley-Tukey FFT algorithm requires storage for 512 complex data points, or 1024 bytes of memory. In the speed measurement system, storage space is necessary for two complete FFT's, or 2K of memory.

A considerable saving in time can be made if the W coefficients are stored in a table and read when required, rather than being calculated as the algorithm suggests. This requires a total of 512 bytes: 256 cos coefficients and 256 sin coefficients.

The TMS32010 supports only 144 bytes of random access memory for the temporary storage of data (RAM), and 4K of Program Memory (PM). It is unfortunate that so little RAM is provided as access to Program Memory takes much longer than access to RAM. Allowing 2K of PM for storage of the signals from the sources and 0.5K for the W coefficients leaves only 1.5K for the actual program. Figure 7.8 shows the allocation of Program memory space for the Signal Processor.

PROGRAM MEMORY	000 (0)
COS COEFFICIENTS	600 (1536)
SIN COEFFICIENTS	700 (1792)
REAL PART OF FIRST DATA SET	800 (2048)
IMAG PART OF FIRST DATA SET	A00 (2560)
REAL PART OF SECOND DATA SET	C00 (3072)
IMAG PART OF SECOND DATA SET	E00 (3584)
	FFF (4096)

FIGURE 7.8 PROGRAM MEMORY ALLOCATION IN THE TMS32010 PROCESSOR

### 7.5.1.3 DATA REPRESENTATION

The data samples read in to the signal processor from the A/D converter are positive, unsigned integers. These samples must be converted to 2's complement bipolar fractions for use in the signal processing algorithm.

The W coefficients stored in the table in Program Memory are also stored in fractional form.

### 7.5.2 TMS32010 CODE

#### 7.5.2.1 SOFTWARE LISTING

The assembled TMS32010 software used in the speed measuring instrument is shown in Appendix C. No description of the TMS32010 instruction set is given here as this may be found in the TMS320 User's Guide [19].

Besides the main program, the Signal Processing Software consists of 15 subroutines. A brief description of the function of each subroutine will be given in the following Section.

#### 7.5.2.2 SUBROUTINE DESCRIPTIONS

- I. MAIN PROGRAM : The main program simply calls the subroutines sequentially. The Main Program is included for clarity.
  
- II. TRANS : This routine transfers constants stored in Program memory into Random Access Memory. It is necessary as PM is non-volatile (stored in EPROM), while the contents of RAM are lost at power-down.

- III. READ1 : This routine toggles the multiplexor to read signals from Source 1. It also sets the current data pointer, CURDAT, to work with the first data space only.
- IV. READ2 : Same as READ1, but for Source 2 and the second data space.
- V. READ : This routine reads in data from the A/D, windows the data, computes the bit-reverse address and stores the data at the bit-reversed address in memory. As the A/D converter operates independantly from the processor, and 'interrupts' the processor when it is ready to transfer data, there is sufficient time to compute the windowing and bit-reversing functions. If no computation were done at this stage, the processor would sit idle waiting for the A/D converter to signal it was ready to transfer data, and thus wasting valuable processing time. This is the reason the form of the FFT algorithm was chosen that requires data to be input in bit-reversed form, rather than applying the bit-reversing at the end of the algorithm.
- VI. FFT1 and FFT2 : As with READ1 and READ2, these routines simply point the current data pointer to the required data space in preparation for the FFT.
- VII. BITREV : This routine 'bit-reverses' the address presented to it. In order to do this, bit manipulation of the address is necessary. With TMS32010 code, bit manipulation is not easy, and the routine is long. Fortunately this routine is called from the READ routine where there is excess time available, and BITREV does not limit the processing speed.

- VIII. FFT : The FFT algorithm closely follows the flowchart of Figure 7.6. As stated in Section 7.3, the 'W' coefficients are stored in a table and read as necessary. WC is the counter used to read the 'W' values. The critical blocks of the algorithm [see Section 7.5.1.1] require only 42 instructions.
- IX. CONV : This routine converts the result of the FFT to the "Power Spectra" as shown in Section 7.4.5.
- X. MULT : The multiply routine multiplies the Power Spectra from the Two Sources together. It only operates on the first 256 data points as the second 256 are redundant as shown in Section 7.1.4.
- XI. MAX : This routine finds the speed (frequency) with the maximum amplitude in the Power Spectrum resulting from the MULT routine.
- XII. ADJ : The purpose of ADJ is to zero the maximum amplitude point in the spectrum before re-applying MAX in order to find the second highest speed. It was found necessary to zero not only the maximum amplitude point but also the points on either side of it.
- XIII. STON : This routine computes the 'Signal-to-noise' ratio of the resultant speed. It does this by measuring the difference between the highest and second highest amplitudes.
- XIV. BTOD : The Binary to Decimal conversion routine converts the maximum amplitude speed to a form that can be used by the display card. As with the BITREV routine, BTOD requires bit manipulation not supported by the TMS32010 code. For this reason the BTOD routine is

extremely inefficient. BTOD is called only once per complete speed measurement and so does not contribute significantly to the computation time.

XV. DSO : This routine switched off the display if the 'signal-to-noise' ratio is less than the preset minimum, MINSN. Because bit 8 of the display can only be switched off by zeroing this bit, DSO writes zero to the output before switching off the display.

### Y7.5.3 PROCESSING SPEED

When the software was tested, it was found that it took 36ms to perform one 512-point FFT. The time required to make a complete speed measurement, from reading in the data to displaying the vehicle speed, was found to be approximately 125ms. Thus the signal processor is capable of making 8 complete speed measurements per second.

## CHAPTER 8 : SPEED MEASURING INSTRUMENT OPERATION

### 8.1 INTRODUCTION

It is the purpose of this chapter to compare the performance of the practical instrument, described in Chapters 4 to 7, to the theoretical performance of the instrument discussed in Chapter 3. Failings of this particular implementation of the proposed system are discussed, and the shortcomings of the system itself are identified.

In the final Section of this chapter some possible improvements to the system are suggested.

### 8.2 INSTRUMENT PERFORMANCE

#### 8.2.1 TEST CONFIGURATION

The speed measuring instrument was tested with the operator and signal processing unit stationed between the instruments, as shown in Figure 8.1. This had the advantage that the operator was close to the 'capture area', and could easily identify which vehicle's speed was being measured. This was especially true when vehicles were travelling close together, and the ability of the instrument to differentiate vehicles was being investigated.

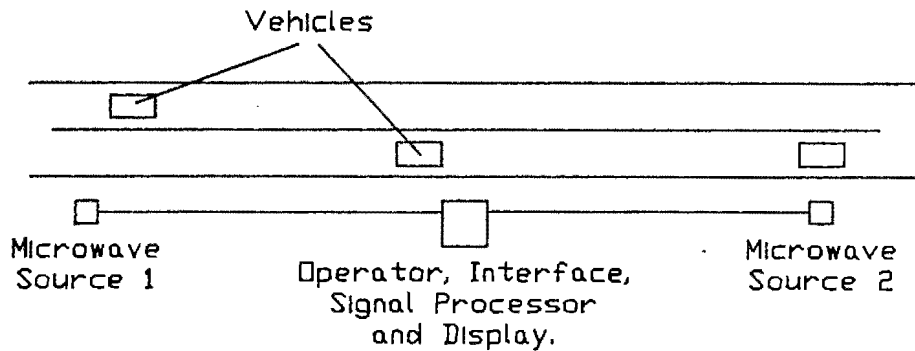


FIGURE 8.1 SPEED MEASURING INSTRUMENT TEST CONFIGURATION

As explained in Section 7.3.1 a portable computer, an Olivetti M10, was used in the speed measuring instrument field tests. It was found that very few adjustments had to be made to the software, the main adjustment being to the value of MINSN, the minimum acceptable 'signal-to-noise' ratio.

The performance of the instrument is evaluated in the following Sections.

### **8.2.2 MEASURED CAPTURE RANGE**

Measurement of the exact size of the capture area is not an easy task. For this reason only the points in each lane at which the speed of vehicles was first measured was recorded. Figure 8.2 shows the approximate size of the measured capture area for vehicles travelling at 100km/h. This measurement was made on a dual carriageway where the speed limit was 120km/h. The two sources were 70m apart.

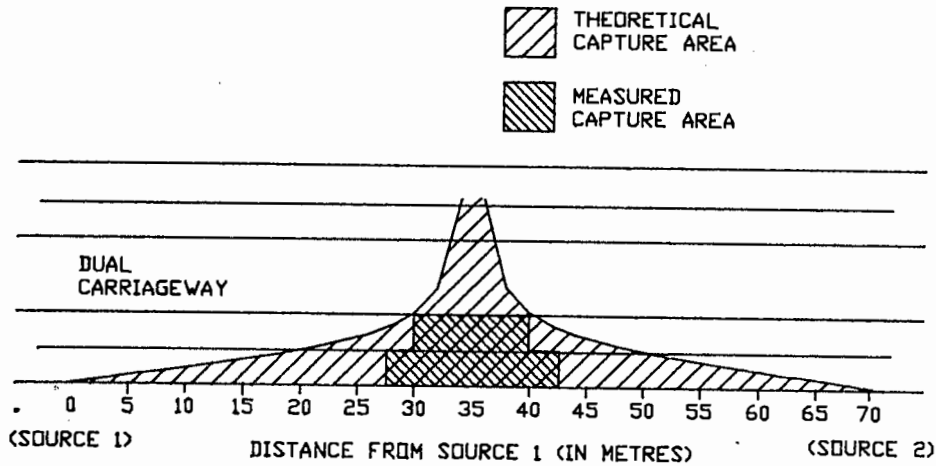


FIGURE 8.2 MEASURED CAPTURE AREA

As can be seen from Figure 8.2, the width of the capture area in the furthest lane is smaller than in the near lane. This was expected as shown by the theoretical capture area which is superimposed on the measured one in Figure 8.2. As can be seen, no portion of the capture area existed in the two lanes carrying traffic in the opposite direction.

It can also be seen that the measured capture area is smaller than the theoretical one. An explanation for this is given in Section 8.3.1.

### **8.2.3 VEHICLE DISCRIMINATION**

As with the measurement of the capture area, an exact measurement of the ability of the instrument to discriminate between vehicles is not trivial. In all the tests done by the author, discrimination between vehicles travelling at 100km/h was always possible if the vehicles were travelling more than 20m apart ( $L=70m$ ). This is the approximate size of the capture area in the closest lane for  $L=70$  and  $s=100km/h$  (see Figure 8.2), thus confirming the assumption

that the target resolution is dependant upon the size of the capture area.

#### **8.2.4 SPURIOUS SPEED READINGS**

If the value of MINSN, the minimum acceptable signal-to-noise ratio, was set too low, spurious speed readings resulted. Conversely, if the value of MINSN was set too high, speed readings were made only when the amplitude of the doppler signals was large.

It was found that to eliminate any spurious speed readings it was necessary to set MINSN to a value of 5000. Even though this value is high, the instrument did not appear to 'miss' many opportunities to make a speed reading.

Because MINSN is simply a linear difference, it is difficult to relate MINSN to an actual value for the signal-to-noise ratio. The actual signal-to-noise ratio allowed by the system is dependant on the amplitude of the largest signal present. The advantage of this representation was that it was easy to set the minimum absolute signal amplitude for which the instrument displayed a vehicle speed.

The causes of spurious speed readings are discussed in Section 8.3.3.

#### **8.2.5 SIGNAL FLUCTUATIONS**

No facility was provided on the prototype instrument for the 'locking', or holding of the display. This is a feature that is found on all commercially available doppler instruments. The lack of this facility actually proved useful as 'dips', or cancellations in the doppler signals could be seen as momentary blanking of the display when a single vehicle was present in the 'capture area'. The

causes of phase cancellations are discussed in Section 8.3.4.

### 8.3 DEVIATION FROM THEORETICAL PERFORMANCE

#### (DUE TO THE PARTICULAR SYSTEM IMPLEMENTATION)

##### 8.3.1 FACTORS AFFECTING THE SIZE OF THE CAPTURE AREA

There are at least three other factors besides the 'cosine error' which affect the size of the measurement zone of the instrument. They are :

- (i) Data record measurement times : Data 'records' of the doppler signals from the sources are read at certain times only. At all times in between the record measurements, the doppler signals are ignored. As shown in Figure 8.3, a record of the signals from each source is made approximately every 80ms. A vehicle travelling at a speed of 200km/h has travelled 4.4 metres in 80ms. If a vehicle has not quite entered the capture area at the end of the measurement of the last data record, the vehicle will already be 4.4 metres inside the capture area at the start of the next data record. It can be seen that this can considerably reduce the apparent size of the capture area, and places a restriction on the minimum length  $L$  between the sources.

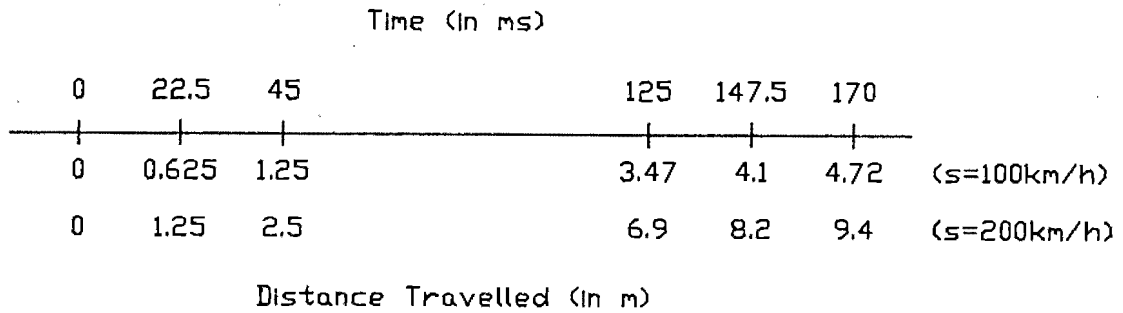


FIGURE 8.3 DATA MEASUREMENT AND SPEED CALCULATION TIMES

(ii) Integral Speed 'Rounding' : The speed resolution of the signal processing software is 1km/h. All speed measurements are effectively 'rounded' during the Fourier Transform. Thus a signal with a speed (frequency) of 68.3 km/h will have most of its power at the 68km/h frequency point. A signal with a speed of 68.8 km/h, on the other hand, will have most of its power at the 69km/h point. Therefore, although the speeds are within 1km/h of each other, they will not correlate. This factor effectively decreases the size of the capture area.

(iii) Spectral Smearing : Spectral smearing can either increase the size of the capture area, or decrease it, depending on the 'severity' of the smearing. The causes of smearing and its effect on the size of the capture area are discussed in Section 8.3.2.

Except for one of the effects of spectral smearing, all of the above factors effectively reduce the size of the capture area. This accounts for the discrepancy between the theoretical and 'measured' capture areas shown in Figure 8.3.

The existence of a finite data record, discussed in (i) above, explains why no part of the capture area exists in the lanes carrying traffic in the opposite direction in Figure 8.2. Although in theory there is a small area in which the convolution of the signals is non-zero, the vehicle is not in this area long enough for the instrument to make a speed measurement.

### 8.3.2 SPECTRAL SMEARING

There are basically two causes of spectral smearing in the speed measuring instrument :

- (i) Close proximity of vehicle to antenna : As shown in Section 5.7.2, when a vehicle passes close to one of the antennas its doppler spectrum is smeared. This causes a reduction in the apparent signal-to-noise ratio which results in no speed measurement being made, and thus reduces the size of the capture area.
- (ii) Windowing : It was shown in Section 7.2.2 that one of the effects of windowing is to 'smear' each spectral line. In the prototype instrument this smearing was reduced, but not eliminated, by the use of a non-rectangular window. With the window described in Section 7.4.4, 'leakage' of power from a frequency point  $f$  occurs into points  $(f-1)$  and  $(f+1)$ . This is the reason it was necessary when calculating the 'signal-to-noise' ratio to disregard the amplitude of points  $(f-1)$  and  $(f+1)$  [Section 7.5.2]. The most serious consequence of this is that it reduces the accuracy of the system to  $\pm 1\text{km/h}$ . A further effect of this smearing is that it increases the size of the capture area. This increase in size is swamped, however, by the factors discussed in Section 8.3 which reduce the size of the capture area.

### 8.3.3 CAUSES OF SPURIOUS SPEED READINGS

In addition to the normal causes of unwanted doppler signals associated with Microwave Doppler SMI's [Appendix A], there are a number of other factors in the prototype instrument which can cause spurious speed readings to be displayed. These factors must be divided into those that are caused by the instrument and those that occur as a result of a particular configuration of vehicles on the road. In this Section only spurious readings caused by the instrument itself (assuming ideal measuring conditions on the road) are considered.

The instrumental causes of spurious speed readings are :

- (i) Noise correlation : It is possible that the random noise generated by one of the microwave sources can correlate at a certain frequency (speed) either with the noise from the other source, or, more likely, with a genuine doppler signal from a vehicle that is not in the capture area. This results in the power at this frequency point being of a higher amplitude than the surrounding noise. Such accidental correlation could cause the 'noise' at this frequency to appear to the instrument as a vehicle that is inside the capture area, whose speed must be displayed. Fortunately the resultant 'signal-to-noise' ratio at this frequency is always relatively low, and it was found that it was possible to completely eliminate spurious readings due to noise correlation by setting MINSN to any value greater than 20.
  
- (ii) Generation of Harmonics : Harmonics of the doppler signals generated can correlate with genuine doppler signals or other harmonics, so causing erroneous readings. Harmonics are generated in the instrument by the mixers and by the instrument amplifiers.

Mixers are inherently non-linear devices, and thus harmonic generation by the mixers is inevitable, particularly when the amplitude of the doppler signals is large. The harmonics produced by mixers are generally low order harmonics, with the second harmonic being by far the largest.

The amplifier most likely to produce harmonics is the second stage of amplification in the doppler pre-amplifier [Section 6.2]. The amplifiers generate harmonics from the doppler signals in two ways : from saturation (clipping), and from slew-rate limiting. Saturation of the amplifiers occurs when the amplitude variation in the doppler signals exceeds the dynamic range of the instrument. In the worst case, a sine wave fed into the amplifier would appear at the output as a square wave. If the sine wave had amplitude  $A$  and frequency  $f$ , then the third harmonic of the square wave would have frequency  $3f$  and amplitude  $A/3$ . If this harmonic fell within the doppler bandwidth of the instrument, it would appear in the frequency spectrum as a vehicle. Other odd harmonics would also be generated, but the third is the most intrusive.

When an amplifier slews, its output cannot follow the change at its input. In the worst case, a sine wave at the input of the amplifier would appear at the output as a triangular wave. Using the same notation as above, the third harmonic of the triangular wave has amplitude  $A/9$ , and thus harmonic generation due to slew-rate limiting is not in general as serious as that due to clipping.

### 8.3.4 CAUSE OF SIGNAL AMPLITUDE FLUCTUATIONS

Phase cancellations in Microwave Doppler instruments occur as a result of the reflected microwave signal taking more than one path on its return to the receiver. An example of this is shown in Figure 8.4. If the difference in the path length is  $(2n+1)\lambda/2$ , where  $n$  is an integer, and the signal amplitudes along each path are the same, total phase cancellation occurs as a result of the superposition of the signals. In practice total cancellations are unlikely; more common is sudden extreme drops in the amplitude of the doppler signal. As shown in Section 6.4.1, the AGC in the instrument cannot track rapid fluctuations, and such 'dips' cause the signal-to-noise ratio to drop suddenly, resulting in the blanking of the display by the instrument.

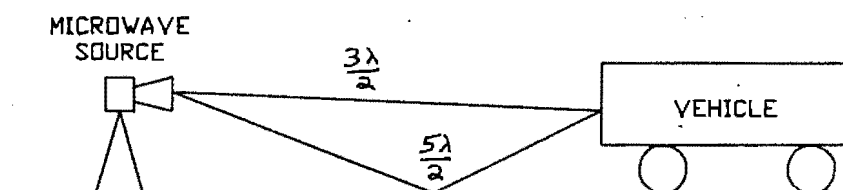


FIGURE 8.4 PHASE CANCELLATIONS DUE TO DIFFERENT PATH LENGTHS

### 8.4 SYSTEM SHORTCOMINGS

There were a number of situations in which the speed measuring instrument failed to perform as expected. These situations are tabulated below :

- (i) More than one vehicle in the capture area : There were a number of occasions where there was more than one

vehicle in the capture area and the instrument continued to display a speed reading. This can occur if both vehicles are travelling at the same speed, or if one vehicle reflects far less of the signal than the other. In such cases it is not known which vehicle's speed is being measured.

- (ii) Displaying a speed when no vehicle was in the capture area : There is a certain configuration of vehicles, shown in Figure 8.5, which causes the instrument to display a speed when there are no vehicles present in the capture area. One vehicle is 'seen' by each source. If the vehicles are travelling at the same speed, the situation will appear to the instrument as one vehicle lying inside the capture area.

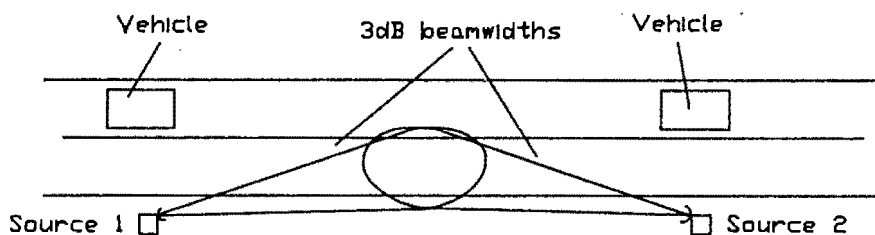


FIGURE 8.5 VEHICLE CONFIGURATION WHERE SPEED MEASUREMENT SYSTEM FAILS

- (iii) Very long vehicles : When a very long vehicle, such as a flatbed trailer, passes through the capture area, its spectral line is radically 'smeared'. This occurs as a result of 'moving phase centres' [Section 5.6] across the vehicle. The spectral smearing degrades the signal-to-noise ratio to such an extent that no speed measurement is displayed.

In contrast to the instrument problems discussed in Section 8.3, the above failings are all faults of the system itself. No cure for these problems is possible unless the proposed system is altered.

## 8.5 POSSIBLE IMPROVEMENTS TO THE SYSTEM

Most of the possible improvements that can be made to the instrument described in Chapters 5 to 7 relate to improving the accuracy of the instrument.

The speed measurement accuracy of the instrument is  $\pm 1\text{km/h}$ . This could be improved by decreasing the frequency resolution of the Fast Fourier Transform. This would require the sampling and storage of a greater number of data points. If more data was stored, the available memory of the TMS32010 would be exceeded, unless a more efficient FFT Algorithm was used [37,38]. Another way of storing more data would be to use a newer, 3rd generation Signal Processor, such as the TMS320C25. Not only can this processor address 128k of data or program memory space, it also runs faster than the TMS32010.

If two or more speed readings were 'averaged', it may be possible to improve the speed accuracy of the instrument, reduce the occurrence of spurious speed readings and eliminate the blanking of the display caused by signal fluctuations. Because of the increase in speed measurement time that this would cause, however, it would probably be necessary to increase the distance  $L$  between the sources (and so increase the size of the capture area) to avoid the problem of 'missing' vehicles discussed in Section 8.3.1.

In order to avoid the system shortcomings described in Section 8.4, it may be possible to include in the system a third doppler sensor at some point between the two sources. This technique has not be investigated by the author.

## CHAPTER 9 : CONCLUSION

In this dissertation a review of existing methods for measuring vehicle speeds by Microwave Doppler Techniques was made. These instruments were shown to have one major flaw : they could not be used in multiple vehicle situations. This problem has led to the virtual disuse of these instruments in South Africa, despite their advantages over other available methods for measuring vehicle speeds.

A new system for measuring vehicle speeds using Microwave Doppler Techniques was presented. This technique was aimed specifically at alleviating the so-called 'vehicle identification' problem. The theory behind the technique was developed and the proposed system was shown to have a relatively small 'capture area.' It was shown that in theory the new system largely overcomes the identification problem.

In order to verify the theoretical performance of the proposed system, the design of a practical speed measuring instrument was described. The instrument design was divided into three sections : The Microwave Sources, the Signal Processor and the Interfacing circuitry.

It was shown that in this instrument the Microwave Source design was far less critical than in Conventional Instruments. A complete design of the Microwave Source (oscillator and mixer) was presented.

The Signal Processor was shown to be a crucial part of the proposed system. The prototype instrument incorporated the TMS32010 dedicated signal processor, chosen because of its speed, flexibility and low cost.

In the Interfacing circuitry both the Automatic Gain Control amplifier and the Anti-aliasing filter were identified as 'critical' components.

When tested the instrument performed largely as expected. The measured capture range was found to be smaller than theoretically predicted. The ability of the instrument to discriminate between vehicles was found to be dependant on the size of the capture area, as expected. The incidence of spurious speed readings was found to be extremely low, far lower than in conventional speed measuring instruments.

In the final section of the dissertation the deviation of the practical from the theoretical performance of the instrument was investigated.

It has been shown that the proposed instrument for measuring vehicle speeds by Microwave Doppler Techniques is a considerable improvement over existing instruments. It is concluded that this instrument has a place in the field of Vehicle Speed Measurement.

## REFERENCES

- (1) E. Belohoubek, "Radar Control for Automotive Collision Mitigation and Headway Spacing", IEEE Trans on Veh. Technol., Vol VT-31, No. 2, May 1982.
- (2) L. Saxton, "Automated Highway System - Considerations for Success", Proc. 30th Annual IEEE Veh. Technol. Conf., Dearborn, MI, Sept 15-17, 1980.
- (3) L. Nagy, J. Lyon, "An Ultrashort Pulse Radar Sensor for Vehicular Precollision Obstacle Detection", IEEE Trans on Veh. Technol., Vol vt-24, No. 4, Nov. 1975.
- (4) R. Mayhan, R. Bishel, "A Two-frequency Radar for Vehicle Automatic Lateral Control", IEEE Trans. on Veh. Technol., No. 1, Feb 1982.
- (5) J. Barker, "Radar, Acoustic and Magnetic Vehicle Detectors", IEEE Trans. Veh. Technol., Vol VT-19, pp 30-43, Feb 1970.
- (6) M. Ross, "Laser Applications - Vol 1", Academic Press, 1971, pp 119-120.
- (7) F. Arrechi et Al, "Laser Handbook - Vol 1", North-Holland, 1972.
- (8) K. Jakus, D. Coe, "Speed Measurement Through Analysis of the Doppler Effect in Vehicular Noise", IEEE Trans on Veh. Technol., Vol VT-24, No. 3, Aug 1975.
- (9) P. Fisher, "Shortcomings of Radar Speed Measurement", IEEE Spectrum, pp 28-31, Dec 1980.

- (10) W. Bojsa, "Police Radar - A time for Constructive Review.", *Microwaves*, p 42, Apr 1980.
- (11) D. Mennie, "Helping Speeders beat the Radar rap", *IEEE Spectrum*, Vol 15, pp 38-42, Aug 1978.
- (12) S. Moshowitz, "Police Radar misses target in Court", *Microwaves*, July 1979.
- (13) J. Brereton, "Stop - Police!", *Motor*, April 1981, pp35-50.
- (14) B. van der Riet, "An Investigation of the Integrity of the Doppler Radar Measurement of Vehicle Speeds, with particular reference to the Digidar 1-K Instrument", NITR division of CSIR, 5 January 1979.
- (15) Operating Manual, Digidar I-K.
- (16) Operating Manual, Digidar II-K.
- (17) R. Dettmer, "Digital Signal Processors", *Electronics and Power*, Feb. 1986.
- (18) 2920 Analog Signal Processor Design Handbook, Intel Corporation, August 1980.
- (19) The TMS32010 User's Guide, Texas Instruments, Texas Instruments Inc., 1983.
- (20) J. Gunn, "Microwave Oscillations of Current in Group III-V Semi-conductors", *Solid State Consm.*, Vol I, pp 88-91, Sept, 1963.

- (21) J. Gunn, "Instability of Current and potential distribution in GaAs and InP., Conf. of Physics on "Plasma Effects in Solids", pp 199-207, 1964.
- (22) B. J. Downing, "Mechanically and Varactor Tuned Gunn Oscillators", M.Sc. Thesis, November 1970.
- (23) D. Cawsey, "Wide-Range Tuning of Solid-State Microwave Oscillators", IEEE J. Solid State Circuits, 1970, pp 82-84.
- (24) Alpha, "Microwave Semiconductors", Alpha Industries Inc., 1983, pp 8.68-8.69.
- (25) M. Lazarus et Al, "A sensitive Millimetre Wave Self-oscillating Gunn Mixer", Proc. of IEEE, Lett., May 1971.
- (26) M. Lazarus et Al, "New Millimetre Wave Receivers using Self-oscillating Gunn Mixers", Microwave Journal, July 1971.
- (27) W. Robins, "Phase Noise in Signal Sources", 1982 Peter Peregrinus on behalf of IEE, Appendix V.
- (28) Skolnik, "Radar Handbook", pp 16-2 to 16-6, McGraw-Hill Book Company, 1970.
- (29) J. Andersen, "Doppler Spectrum of Single Automobiles", IEEE Trans. on Veh. Technol., Vol VT-31, No. 1, Feb 1982.
- (30) H. Friis, "Noise Figure of Radio Receivers", Proc. of IRE, July 1944, pp 419-422.
- (31) G. Clayton, "Data converters", Macmillan Press, London, 1982, pp 87-92.

- (32) L. Bruton, "Network Transfer Functions using the concept of Frequency Dependant Negative Resistance", IEEE Trans. on Circuit Theory, Aug 1969.
- (33) S. Nandi, P. Jana, "Floating Ideal FDNR using Current Conveyors", Electron. Lett., Vol 19, p 251, 1983.
- (34) R. Senani, "Floating Ideal FDNR using only two current conveyors", Electron. Lett., March 1984, Vol 20, No. 5.
- (35) Z. Ali, "FFT Algorithms Speed Digital Signal Processing", Electronic Design, July 1980.
- (36) S. Magar, R. Hester, R. Simpson, "Signal Processing Microcomputer Builds FFT-based Spectrum Analyser", Electronic Design, August 1982.
- (37) J. Martens, "Discrete Fourier Transform Algorithms for Real Valued Sequences", IEEE Trans. Acoust., Speech, Signal Processing, Vol ASSP-32, No. 2, pp 390-396, April 1984.
- (38) G. Bergland, "A Fast Fourier Transform Algorithm for Real Valued Series", Commun. ACM, Vol 11, pp 703-710, Oct 1968.
- (39) G. Bergland, "A Guided Tour of the Fast Fourier Transform", IEEE Spectrum, July 1969.
- (40) R. Blackman, J. Tukey, "The measurement of Power Spectra", New York, Dover, 1958.
- (41) J. Kaiser, "Non-recursive Digital Filter Design using the  $I_0$ -sinh Window Function", Proc. 1974 IEEE Symposium on Circuits and Systems, San Francisco, Apr. 1974, pp 20-23.

- (42) J. Cooley, J. Tukey, "An Algorithm for the Machine Calculation of the Complex Fourier Series", Math. Comput., Vol 19, pp 297-301, Apr. 1965.
- (43) P. Duhamel, H. Hollman, "Split-Radix FFT Algorithm", Electron. Lett., Vol. 20, pp 14-16, 1984.
- (44) S. Prakash, V. Rao, "A new Radix-6 FFT Algorithm", IEEE Trans. Acoust., Speech, Signal Processing, Vol ASSP-29, pp 939-941, Aug 1981.
- (45) E. Dubois, A. Venetsanopoulos, "A new Algorithm for the Radix-3 FFT", IEEE Trans. Acoust, Speech, Signal Processing, Vol ASSP-28, pp 205-215, Apr 1980.

APPENDIX A

A SUMMARY OF THE FINDINGS OF THE CSIR REPORT TITLED :

"AN INVESTIGATION OF THE INTEGRITY OF THE DOPPLER RADAR  
SPEED MEASUREMENT OF VEHICLE SPEEDS" [14].

(REPRINTED FROM THE CSIR REPORT).

CLASS OF ERROR	CAUSE	CRITICAL FACTOR	CORRECTIVE MEASURES	
Errors of Accuracy	Incorrect Doppler frequency	Trigonometrical error which occurs if radar is not on vehicle's velocity vector	Readings always low so care necessary when enforcing minimum speed limits	
		Radar wavelength ( $\lambda$ )	Calibrate $\lambda$ Genuine Speed Calibration	
Errors of identification	Inaccurate conversion of Doppler frequency to speed	Counter time-base (T)	Calibrate T	
		Quantization error	None (Display has too few digits)	
	Inability to guarantee accuracy	Specified calibration procedures	Establish correct procedures	
	Non-Doppler signals	Internal electrical interference	Faulty electronics	Service or repair
		External electromagnetic interference	Proximity to other transmitters	Avoid other transmitters
		Vapour discharge lamps	Street lights in radar beam	Poses no problem but avoid
		Vibration of portions of the target	Mechanical details of the target	Foses no problem
	Non-vehicular	Stationary rotating machinery	Vibration of the radar antenna	Poses no problem but avoid
			Trees, birds, insects, flapping tarpaulins, etc.	Should pose no problem but avoid
	Doppler signals	Antenna sidelobes irradiating other moving vehicles	Position in the radar beam and distance relative to that of suspect vehicle	They pose no problem
Antenna design or mechanical damage			poses no problem	
Vehicular signals	Portions of vehicle moving faster, e.g. cooling fans, hub caps	Mechanical details of these items	They pose no problem	
		Relative distances and scattering polar diagrams of vehicle and objects	Poses no problem	
	Unexpected deflection of part of the radar beam into other direction	Large plane reflectors in radar beam	Choose sites without such reflectors	
		Their relative positions and scatter cross-sections	Avoid at all costs	
Speed reading held over from previous measurement	Display time of speed reading	Operator to be alert to problem		

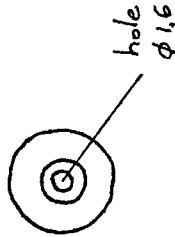
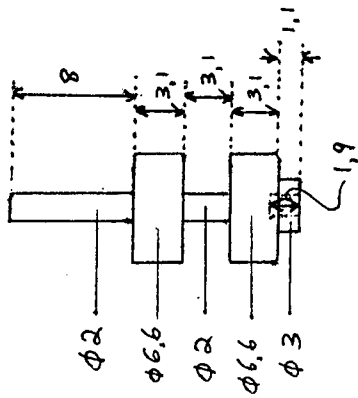
TABLE 3: ERROR MODES OF DOPPLER RADAR SPEED METERS

**APPENDIX B**

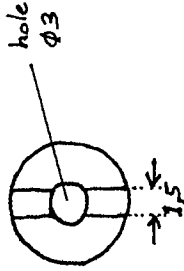
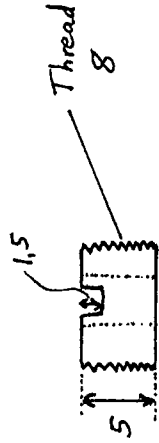
**DIAGRAMS FOR THE CONSTRUCTION OF THE MICROWAVE SOURCE,  
ANTENNA AND ACCESSORIES.**



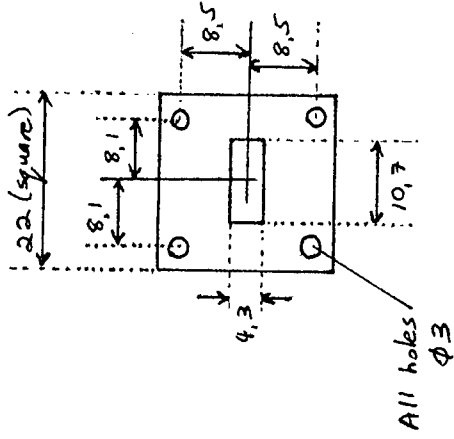
MICROWAVE CHOKE



MICROWAVE CHOKE SUPPORT



SPACERS



Thicknesses : 0,5, 1, 2, 4, 8.

All dimensions m.m.

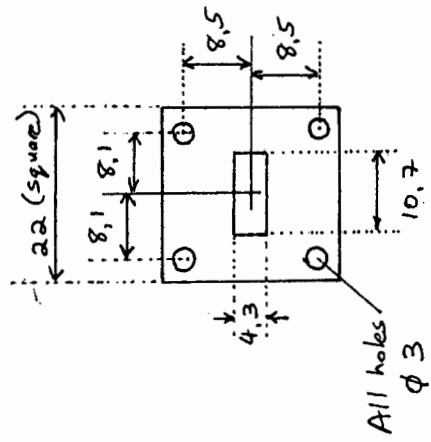
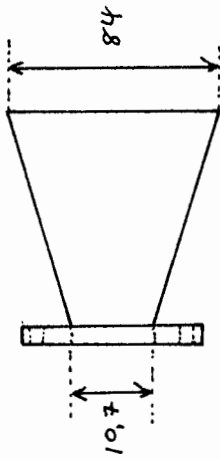
MICROWAVE SOURCE  
ACCESSORIES

NEIL MARTIN

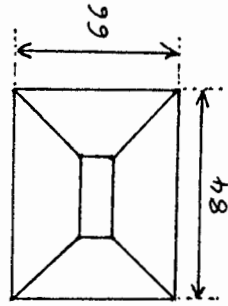
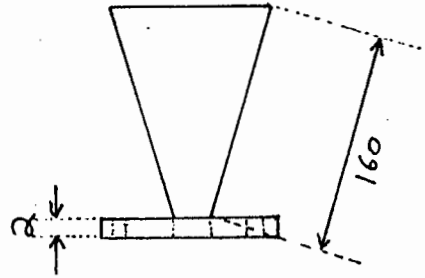
DRAWING 2 OF 3

3/9/85

1 m.m. brass  
except flange (2 m.m.)



All holes  $\phi 3$



HORN ANTENNA	Version 2
NEIL MARTIN	29/8/85
DRAWING 3 OF 3	2 Required

All dimensions m.m.

APPENDIX C

TMS32010 SOFTWARE FOR THE DOPPLER SPEED MEASUREMENT SYSTEM



MINSN	EQU	16	Minimum allowable 'Signal to Noise' ratio
BIT	EQU	17	Variable used in Bit Reversing Routine
ORIG	EQU	18	Variable used in Bit reversing Routine
K	EQU	19	Index K used in FFT Algorithm
M	EQU	20	Index M used in FFT Algorithm
I	EQU	21	Index I used in FFT Algorithm
J	EQU	22	Index J used in FFT Algorithm
XRI	EQU	23	Real Part of x(I)
XII	EQU	24	Imag Part of x(I)
XRI2	EQU	25	Real Part of x(I2)
XII2	EQU	26	Imag Part of x(I2)
WR	EQU	27	Real Part of W
WI	EQU	28	Imag Part of W
WC	EQU	29	Counter used to fetch W values from look-up table
BR	EQU	30	Variable used in FFT Butterfly
BI	EQU	31	Variable used in FFT Butterfly
TEMP1	EQU	32	Temporary storage variable
TEMP2	EQU	33	Temporary storage variable
I2	EQU	34	
DUMMY	EQU	35	Dummy variable
CURDAT	EQU	36	Current data pointer
PORT	EQU	37	External Port Address
ADDR	EQU	38	Address Value
XM	EQU	39	Magnitude of x
COUNT	EQU	40	Counter variable
UNITS	EQU	41	Units variable used in Binary to Decimal Conversion
TENS	EQU	42	Tens variable used in Bin to Dec Conversion
HUNS	EQU	43	Hundreds variable used in Bin to Dec Conversion
SPEED	EQU	44	Speed variable
SPVAL	EQU	45	Speed Amplitude
TVAL	EQU	46	Temporary storage variable
TSPEED	EQU	47	Temporary storage variable
SN	EQU	48	'Signal to noise ratio' variable.

```

*
*
*****
*                                     *
*                               DATA RAM INITIALISATION                               *
*                                     *
*****
*
*

```

DSTART	DATA	512	Number of points = 512 (N)
	DATA	9	L2N=9
	DATA	0	Array
	DATA	>05FF	Start of cos data - 1
	DATA	>06FF	Start of sin data - 1
	DATA	>07FF	Start of Re part of first data set - 1
	DATA	>09FF	Start of Im part of first data set - 1
	DATA	>0BFF	Start of Re part of second data set - 1



```

*****
|
|                                     |
|                               TRANSFER ROUTINE                               |
|                                     |
|*****
|
TRANS  LACK  1
        SACL  1          Set 'One' = 1 for use in this routine
|
        LACK  DSTART      Load start address of data to transfer
        LARK  0,0         Zero ARO
        LARK  1,16       Set AR1 as counter
NEXT   LARP  0           Point to ARO
        TBLR  #+         Make Transfer and increase ARO
        ADD   ONE        Increment Accumulator
        LARP  1           Point to AR1
        BANZ  NEXT       Repeat until all data transferred from PM to DM
        RET              Return to Main Program
|

```

```

*****
|
|                                     |
|                               READ1                                       |
|                                     |
|*****
|
READ1  IN    DUMMY,1      Point Multiplexor to Port 1 (Source 1)
|
        LAC   D1REPM      Load Start address of first data memory location
        SACL  CURDAT      Store in 'Current Data' variable
|

```

```

RET
|
*****
|
|                                     |
|                               READ2                                       |
|                                     |
|*****
|
READ2  IN    DUMMY,2      Point Multiplexor to Port 2 (Source 2)
|
        LAC   D2REPM      Load Start Address of Second data location
        SACL  CURDAT      Store in 'Current Data' variable
|
        RET
|
|
|
|
|
|
|

```



```

      ADD    OFFSET
      TBLW   ZERO           Write zero to the corresponding Imaginary part of the data point

      LAC    COUNT
      ADD    ONE
      SACL   COUNT         COUNT = COUNT + 1
      SUB    N             Check if all data read
      BLEZ   LOOP         If not, continue

      RET                    Return to main program

```

```

      ::::::::::::::::::::::::::::::::::::::::::::::::::::::::::::::::::::::::::::::::::::
      BIT REVERSING ROUTINE
      ::::::::::::::::::::::::::::::::::::::::::::::::::::::::::::::::::::::::::::::::::::

```

```

BITREV  ZAC
      LAC    COUNT         COUNT holds address to reverse
      SUB    ONE           Adjust it for entry to this routine
      SACL   ORIG         and store it in ORIG

      LARP   0             ARP = 0
      LAR    0,L2N        Set AR0 = L2N, the number of bits in the address
      BANZ   CONT         Set AR0 = L2N - 1 (Decrement AR0)

CONT    ZAC
      SACL   ADDR         Clear register for bit-reversed address

NOG     LAC    ONE
      AND    ORIG        Mask bit one of original address
      SACL   BIT         and store it.

      LAC    ADDR,1
      ADD    BIT         Add stored address bit to final result
      SACL   ADDR        and restore it.

      LAC    ORIG,15
      SACH   ORIG        Right shift the original address by one

      BANZ   NOG         Repeat until finished.

      LAC    ADDR
      ADD    ONE         Re-adjust address for use in FFT algorithm
      SACL   ADDR        Bit reversed address now stored in ADDR.

      RET                    Return to main program

```



```

        SACL   J           J = 0
*
NEXTJ   LAC     J
        ADD     ONE
        SACL   J           J = J + 1
        SACL   I           I = J
*
NEXTI2  LAC     I
        ADD     M
        SACL   I2          I2 = I + M
*
*
*** Fetch x(I) and x(I2) values from Program Memory ***
*
*
        ADD     CURDAT      Compute address of Real part of x(I2)
        TBLR   XRI2        and store in XRI2
*
        ADD     OFFSET      Compute Address of Imag part of x(I2)
        TBLR   XII2        and store in XII2
*
        LAC     I
        ADD     CURDAT      Similarly fetch Re part of x(I)
        TBLR   XRI
*
        ADD     OFFSET      and Imag part.
        TBLR   XII
*
*
*** FFT Butterfly ***
*
*
        LT     XRI2
        MPY    WR           WR*XRI2
        PAC
        LT     XII2
        MPY    WI           WI*XII2
        SPAC
        SACH   BR,1        BR = WR*XRI2 - WI*XII2
*
        MPY    WR           WR*XII2
        PAC
        LT     XRI2
        MPY    WI           WI*XRI2
        APAC
        SACH   BI,1        BR = WR*XII2 + WI*XRI2
*
        LAC    XRI,15
        SUB    BR,15
        SACH   XRI2        XRI2 = XRI - BR

```

ADDH	BR	
SACH	XRI	XRI = XRI + BR

LAC	XII,15	
ADD	BI,15	
SACH	XII	XII = XII + BI
SUBH	BI	
SACH	XII2	XII2 = XII - BR

\*\*\* Restore new x(I) and x(I2) values in Program Memory \*\*\*

LAC	I2	
ADD	CURDAT	Compute address Real part of x(I2)
TBLW	XRI2	and store XRI2

ADD	OFFSET	
TBLW	XII2	Store XII2

LAC	I	
ADD	CURDAT	
TBLW	XRI	Store XRI

ADD	OFFSET	
TBLW	XII	Store XII

LAC	I	
ADD	K	
SACL	I	I = I + K

SUB	N	Check if I is greater or equal to N
BLZ	NEXTI2	If not, repeat 'I2' loop

\*\*\* Fetch new W coefficients from Program Memory \*\*\*

LT	WC	
MPY	J	Required W coefficient is at address WC*J
PAC		
ADD	COSPM	Add address of stored cos coefficients
TBLR	WR	and store cos coefficient in WR
ADD	DIFF	Add address of stored sin coefficient
TBLR	WI	and store sin coefficient in WI

LAC	J	
SUB	M	Check if J is greater than or equal to M
BLZ	NEXTJ	If not, repeat 'J' loop



```

*****
*                                     *
*                               MULTIPLY ROUTINE                               *
*                                     *
*****
*
MULT   ZAC
      SACL   COUNT           COUNT = 0
*
AGAIN  LAC   COUNT
      ADD   ONE
      SACL  COUNT           COUNT = COUNT + 1
      SUB   DIFF           Check if all data multiplied
      BGEZ  EOM           If it is, end multiply.
*
      LAC   DIREPM
      ADD   COUNT           Compute next XM address from first data set
      TBLR  XM             And fetch XM
      LT    XM
      LAC   D2REPM
      ADD   COUNT           Compute next XM address from second data set
      TBLR  XM             Fetch XM
      MPY   XM
      PAC
      SACH  XM,1           XM = XM (from first set) * XM (second set)
*
      LAC   DIREPM
      ADD   COUNT
      TBLW  XM             Store XM in memory allocated for first data
*
      B     AGAIN         Repeat
EOM    RET
*
*

```

```

*****
*                                     *
*                               MAX SPEED FIND                               *
*                                     *
*****
*
MAX    ZAC
      SACL  COUNT           COUNT = 0
      SACL  SPEED          SPEED = 0
      SACL  SPVAL          SPVAL = 0
*
MIND   LAC   COUNT
      ADD   ONE
      SACL  COUNT           COUNT = COUNT + 1
      SUB   DIFF           Check if all data searched
      BGEZ  CMPLT         If yes, end Max

```



```

+++++
|                                     |
|           'SIGNAL TO NOISE RATIO' MEASUREMENT           |
|                                     |
+++++

```

```

|
|
| STON  LAC  TVAL      Load max amplitude value
|       SUB  SPVAL     Subtract next highest amplitude
|       SACL SN        and store as 'Signal to noise ratio'
|
|       LAC  TSPEED
|       SACL SPEED     Store 'highest amplitude' speed in SPEED
|
|       RET           Return to main program.
|

```

```

+++++
|                                     |
|           BINARY TO DECIMAL CONVERSION                 |
|                                     |
+++++

```

```

|
|
| BTOD  ZAC
|       SACL UNITS     UNITS = 0
|       SACL TENS     TENS = 0
|       SACL HUNS     HUNS = 0
|
|
| REDD  LAC  SPEED
|       SUB  ONE
|       BLZ  FIN      If SPEED - 1 is less than zero then end BTOD
|       SACL SPEED    SPEED = SPEED - 1
|       LAC  UNITS
|       ADD  ONE
|       SACL UNITS     UNITS = UNITS + 1
|       SUB  TEN
|       BLZ  REDD     If UNITS is less than or equal to TEN, repeat
|       ZAC
|       SACL UNITS     Clear UNITS
|       LAC  TENS
|       ADD  ONE
|       SACL TENS     TENS = TENS + 1
|       SUB  TEN
|       BLZ  REDD     If TENS is less than or equal to TEN, repeat
|       ZAC
|       SACL TENS     Clear TENS
|       LAC  HUNS
|       ADD  ONE
|       SACL HUNS     HUNS = HUNS + 1
|       B    REDD     Repeat

```

```

*
FIN   ZAC
      ADD     HUNS,8
      ADD     TENS,4
      ADD     UNITS
      SACL    SPEED          Speed = HUNS + TENS + UNITS in format required by display card
      OUT     SPEED,0        Output speed to Display card.
*
      RET          Return to main program.
*
*****
*
*           DISPLAY SWITCH OFF
*
*****
*
DSO   OUT     0,1           Switch on display
      LAC     SN           Fetch 'Signal-to noise ratio'
      SUB     MINSN        Subtract minimum allowable S/N ratio
      BGZ     EOD          If S/N ratio greater than that allowed, end DSO
*
      OUT     ZERO,0       Write zero to the display
      OUT     0,2          and switch off the display
*
EOD   RET          Return to main program.
*
*****
*
INIT  B       START
INTR  B       START
*
      END

```

**APPENDIX D**

**PART OF THE DATA SHEET OF THE TMS32010**

**PIN NOMENCLATURE**

NAME	I/O	DEFINITION
A11-A0/PA2-PA0	O	External address bus. I/O port address multiplexed over PA2-PA0.
$\overline{BIO}$	I	External polling input for bit test and jump operations.
CLKOUT	O	System clock output, 1/4 crystal/CLKIN frequency.
D15-D0	I/O	16-bit data bus.
$\overline{DEN}$	O	Data enable indicates the processor accepting input data on D15-D0.
$\overline{INT}$	I	Interrupt.
MC $\overline{MP}$	I	Memory mode select pin. High selects microcomputer mode. Low selects microprocessor mode.
$\overline{MEN}$	O	Memory enable indicates that D15-D0 will accept external memory instruction.
NC		No connection.
$\overline{RS}$	I	Reset used to initialize the device.
VCC	I	Power.
VSS	I	Ground.
$\overline{WE}$	O	Write enable indicates valid data on D15-D0.
X1	I	Crystal input.
X2/CLKIN	I	Crystal input or external clock input.

The TMS320 family's unique versatility and power give the design engineer a new approach to a variety of complex applications. In addition, these microcomputers are capable of providing the multiple functions often required for a single application. For example, the TMS320 family can enable an industrial robot to synthesize and recognize speech, sense objects with radar or optical intelligence, and perform mechanical operations through digital servo-loop computations.

**architecture**

The TMS320 family utilizes a modified Harvard architecture for speed and flexibility. In a strict Harvard architecture, program and data memory lie in two separate spaces, permitting a full overlap of the instruction fetch and execution. The TMS320 family's modification of the Harvard architecture allows transfers between program and data spaces, thereby increasing the flexibility of the device. This modification permits coefficients stored in program memory to be read into the RAM, eliminating the need for a separate coefficient ROM. It also makes available immediate instructions and subroutines based on computed values.

The TMS320C10 utilizes hardware to implement functions that other processors typically perform in software. For example, this device contains a hardware multiplier to perform a multiplication in a single 200-ns cycle. There is also a hardware barrel shifter for shifting data on its way into the ALU. Finally, extra hardware has been included so that auxiliary registers, which provide indirect data RAM addresses, can be configured in an autoincrement/decrement mode for single-cycle manipulation of data tables. This hardware-intensive approach gives the design engineer the type of power previously unavailable on a single chip.

**32-bit ALU/accumulator**

The TMS320C10 contains a 32-bit ALU and accumulator that support double-precision arithmetic. The ALU operates on 16-bit words taken from the data RAM or derived from immediate instructions. Besides the usual arithmetic instructions, the ALU can perform Boolean operations, providing the bit manipulation ability required of a high-speed controller.

## APPENDIX E : PUBLISHED WORK AND PATENT

A part of the work included in this dissertation was presented at the conference : "Joint Symposium on Antennas and Propagation and Microwave Theory and Techniques", on 19, 20 and 21 August 1986 held at the CSIR in Pretoria.

It was presented under the Title : "A Novel Doppler Technique for Vehicle Speed Determination", by N C Martin and B J Downing.

A Provisional Patent on the material covered in this dissertation has been filed. The patent is held jointly by: The University of Cape Town and Plessey S.A., with inventors N C Martin and B J Downing.